NPS ARCHIVE
1960
INMAN, R.

NONLINEAR REACTANCE HARMONIC GENERATION BY MULTIPLE CONVERSION PROCESS

RICHARD P. INMAN

DUDLEY KNOX LIBRARY
NAVAL POSTGRADUATE SCHOOL
MONTEREY, CA 93943-5101

[illegible]

NONLINEAR REACTANCE HARMONIC GENERATION BY MULTIPLE CONVERSION PROCESS

* * * * *

Richard P. Inman

NONLINEAR REACTANCE
HARMONIC GENERATION
BY MULTIPLE CONVERSION PROCESS

by

Richard P. Inman

Lieutenant, United States Navy

Submitted in partial fulfillment of
the requirements for the degree of

MASTER OF SCIENCE
IN
ENGINEERING ELECTRONICS

United States Naval Postgraduate School
Monterey, California

1 9 6 0

NPS ARCHIVE
1960
INMAN, R

Thesis
~~I52~~

NONLINEAR REACTANCE HARMONIC GENERATION BY MULTIPLE CONVERSION PROCESS

by

Richard P. Inman

This work is accepted as fulfilling
the thesis requirements for the degree of
MASTER OF SCIENCE
IN
ENGINEERING ELECTRONICS
from the
United States Naval Postgraduate School

ABSTRACT

The merits of using multiple conversion processes or modes in practical nonlinear reactance harmonic generators to increase conversion efficiency and power transfer are investigated. In normal operation of harmonic generators only two frequencies are present, the fundamental and the desired harmonic frequency. In the multiple conversion process other frequencies are also present and are terminated in idler circuits.

A Hamiltonian analysis of the multiple conversion process due to Dr. Peter Sturrock, Varian Associates Consultant, is presented.

The experimental work emphasizes the principles of multiple conversion. It shows conclusively that for the third harmonic generator circuit considered -- using square law nonlinear reactance elements -- the conversion efficiency and power transfer are increased. This work also shows that multiple frequency output is feasible.

The writer wishes to express his appreciation for the assistance and encouragement given him by Mr. William Beavers, Dr. Alfred Prommer, Dr. Peter Sturrock, and Mr. A. Norris of Varian Associates and by Professor W. M. Bauer and Professor Raymond Murray of the U. S. Naval Postgraduate School in this investigation.

TABLE OF CONTENTS

Section Title Page

Title Page i
Abstract ii
Table of Contents iii
List of Illustrations iv

1. Introduction to Harmonic Generation

a. General Background 1
b. Nonlinear Reactance Harmonic Generation 4

2. Harmonic Generation by Multiple Conversion Process 7

3. Nonlinear Reactance Harmonic Generation Theory

a. General Discussion of Theory and Methods 10
b. Brief Introduction to Hamiltons Principle 11
c. Nonlinear Circuits Treated by Hamiltonian Methods 13
d. A Solution for the Multiple Conversion Process 19

4. Experimental Circuit Design 25

5. Experimental Results and Conclusions
a. Direct Conversion

1. 3rd Harmonic Generator 30
2. 2nd Harmonic Generator 30

b. Multiple Conversion

1. 3rd Harmonic Generator 33
c. Effects of Idling Circuit Terminations 37
d. Discussion of Losses 40

6. Summary 43

7. Suggested further Investigations 44

8. Bibliography 45

Appendix Title Page

I. Large Signal Analysis of Nonlinear Reactance Harmonic Generator (3rd Harmonic) I-1

II. Evaluation of Diode V vs C Characteristic II-1

III. Evaluation of Diode Energy vs Charge Characteristic III-1

IV. A. Circuit Design Problems IV-A-1
B. Alignment Procedure for 2nd and 3rd Harmonic Generator Circuit IV-B-1

V. Experimental Data V-1

LIST OF ILLUSTRATIONS

Figure	Title	Page
1.	The Manley-Rowe Multiplier Circuit	5
2.	3rd Harmonic Generator Using Multiple Conversion	7
3.	"Parametric" Circuit	18
4.	"Energy Flow" Chart	18
5.	Experimental 2nd and 3rd Harmonic Generator Circuit Diagram	28
6.	Photograph of Experimental Circuit	29
7.	Plot of Direct Conversion 3rd Harmonic efficiency P_3/P_1 vs R_{3L}	30
8.	Plot of Direct Conversion 2nd Harmonic efficiency P_2/P_1 vs R_{2L}, V_1 fixed	31
9.	Plot of Direct Conversion 2nd Harmonic efficiency P_2/P_1 vs V_1 for various R_{2L}	32
10.	Plot of Multiple Conversion 3rd Harmonic Conversion efficiency P_3/P_1 vs R_{3L}, $R_{2L} = 0$, V_1 = const.	33
11.	Plot of Multiple Conversion 3rd Harmonic Conversion efficiency P_3/P_1 vs V_1 for various values of R_{3L}	34
12.	Plot of Multiple Conversion 3rd Harmonic Conversion efficiency P_3/P_1 vs R_{2L} for various R_{3L} for V_1 = const.	37
13.	Plot of P_3 vs R_{2L} for various R_{3L}, V_1 = const.	37
14.	Simplified Multiple Conversion Loss Circuit	41

Appendix Illustrations

Figure		Page
II-A	Diode Characteristic Measuring Circuit	II-1
II-1	Linear Plot V vs C Characteristic for Varicap Diode	II-3
II-2	Log-Plot V vs C Characteristic for Varicap Diode	II-4
III-1	Linear Plot V vs Q for Harmonic Generator Nonlinear Element	III-2
III-2	Linear Plot of V and Q vs V Harmonic Generator Nonlinear Element	III-4
IV-A	Input Impedance - Circuit Diagram	IV-A-2
IV-1	Photograph of Harmonic Generator and Equipment Used	IV-B-3

Introduction to Harmonic Generation

a. General Background

A circuit or system which includes a nonlinear device will produce a frequency response which will include harmonics, or multiples, of the driving force frequency. This is true in mechanical as well as electronic systems. Mathematically this involves either the raising of a trigonometric function, sine or cosine, to a power or powers greater than the first, or by periodically interrupting the trigonometric function.

Throughout the history of electronics it has grown to be a common practice to use harmonic generation to extend upward the usable frequency range when an immediate source of fundamental mode power has not been developed. [1]

Now we are again faced with the problem of extending our frequency spectrum this time into the centimeter and millimeter range where applications of these frequencies are desireable for radio astronomy, microwave spectroscopy [2], special superheterdyne receivers [3], and communications [4]. Present day multiplier devices in the centimeter and millimeter wave region using traveling wave structures, klystrons, magnetrons, etc, have small power output. The following is data on millimeter power output as reported in the Millimeter Wave Conference:

Elliot Brothers,	England	Klystron	8mm	30 watts
CSF,	France	Carcinotron	4mm 2mm	1-2 watts 100-200m watts
Phillips,	Holland	Klystron	4mm	50m watts

In these devices the RF fields tend to shrink closely around the

traveling wave structures and weaken the interaction between the electrons and the RF fields with the resulting effect that the multiplier efficiency of the device is very low. Size limitations are also a problem and have put upper limits on the output frequencies.

Millimeter waves have been generated by other devices including field emission cathode [5], welded contact rectifiers [6], gold bonded germanium diodes [7] and nonlinear capacitance junction diodes [8,9]. The conversion efficiency and the power output of these devices is generally low except for the nonlinear capacitance junction diodes.

Generally we can classify nonlinear devices for harmonic generation in two types: the nonlinear resistance and the nonlinear reactance. Extensive work has been done in the field of nonlinear resistive devices for harmonic generation even up into the millimeter range. However Page [10] has shown that nonlinear resistive devices have a power conversion ratio limit of $1/n^2$, while for ideal rectifiers the power conversion ratio is $1/n^4$. Thus we see that the ideal nonlinear resistance used as a 3rd harmonic generator has a minimum power conversion loss of 9.5db while an ideal rectifier has a minimum conversion loss of 19db. The ideal nonlinear reactance as a harmonic generator as shown by Manley - Rowe [11] delivers all power absorbed from the power source to the load at the harmonic frequency. Thus if we were to have a low loss nonlinear reactance we could expect high conversion efficiency. The parametric or nonlinear capacitance diode is such a device.

The development of the nonlinear capacitance diode stems from the nonlinear resistance crystal diode. It was noted that the equivalent circuit of some of the crystal diodes was a nonlinear barrier resistance shunted by a nonlinear capacitance [6]. At that time this was considered

as an undesirable characteristic of the diode Now with advances in the manufacturing techniques of diodes and junctions of solid state materials brought on by the transistor and other solid state devices the barrier or junction resistances have been reduced to a very low value making the device essentially a nonlinear capacitance. The development of this diode has been spurred by the interest in its use in parametric amplification [8].

At microwave frequencies nonlinear capacitance junction diode harmonic generators have not yet realized the exceedingly high efficiencies predicted by the Manley - Rowe relationships due to diode losses, although results so far do look promising. [8, 9, 12] In analog frequency circuits results approaching optimum have been obtained and theory has been developed which corresponds very closely to these relationships. [13, 14, 15]

1(b)

Nonlinear Reactance Harmonic Generation

Manley and Rowe /11/ have derived the general energy relationships for nonlinear reactive elements that are excited by one or more driving sources. While most of this work is best known for its application to the parametric amplifier problem, it is also applicable to the problem of harmonic generation using nonlinear reactance.

The general relationships derived for mixing applications with a single valued nonlinear reactance characteristic are as follows:

$$\sum_{m=0}^{\infty} \sum_{n=-\infty}^{\infty} \frac{m W_{m,n}}{m f_1 + n f_0} = 0$$

and

$$\sum_{m=-\infty}^{\infty} \sum_{n=0}^{\infty} \frac{n W_{m,n}}{m f_1 + n f_0} = 0$$

Now from these general relationships if we assume the power input $W_{1,0}$ at the fundamental frequency f_1 and the power output $-W_{m,0}$ at the harmonic frequency mf_1, setting all other powers equal to zero, then

$$W_{1,0} = \sum_{m=2}^{\infty} - W_{m,0}$$

Now since it is assumed that the nonlinear reactance is lossless then the total harmonic power output is equal to the fundamental power input. Therefore if the load impedences at the unwanted harmonics can be made to go to zero, infinity, or be purely reactive, the power gain to the desired harmonic can approach unity. This would be a highly desirable condition and if it could be realized would offer such a great increase over the nonlinear resistive elements in theoretical conversion limitations that the nonlinear resistive devices would no longer be used. There are, however, two general problems that limit this

theoretical condition.

One, the Manley-Rowe equations apply to the theoretical ideal lossless reactive element. The only presently available devices which approach this theoretical condition and are suitable for the microwave and millimeter wave regions are the nonlinear capacitance junction diodes. With these diodes is associated a series spreading resistance in which there will be some power loss at both the fundamental and harmonic frequencies. This spreading resistance may be the limiting factor in use of this diode.

Secondly, the relationships derived concern only fundamental power which is absorbed by the reactive element from the source, not the source capability. A high conversion efficiency results in optimum harmonic generation only if a high degree of matching is obtained. This degree of matching attainable may be a practical limitation to the use of the nonlinear reactive element as a harmonic generator.

For the purpose of illustration, the generalized circuit, Figure 1, is shown below. This circuit has been used by Manley - Rowe in Reference 11, and through frequent reference to it has acquired the names of the authors.

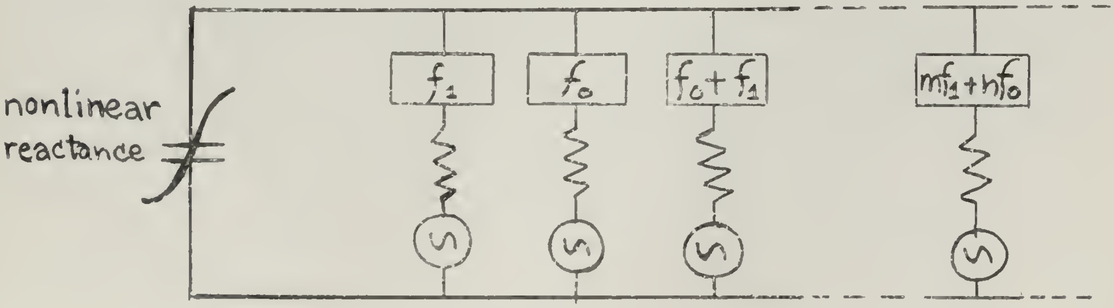

Figure 1

The "Manley - Rowe Multiplier Circuit"

In each branch a filter allows only the current of $mf_1 + nf_0$ to flow, and we see that a source and load may exist in each branch.

Thus it can be seen that the nonlinear capacitance should have a better power conversion efficiency than a nonlinear resistance and should be superior in power handling capability to a similarly constructed nonlinear resistance. For nonlinear capacitance junction diodes, however, there is a peak voltage limitation which is caused by the forward conduction and reverse breakdown regions. If we were to operate in this forward conduction region we have essentially a nonlinear resistive device and our efficiency again drops off as $\frac{1}{n^2}$.

Harmonic Generation by Multiple Conversion Process

Manley-Rowe have shown that the theoretical conversion loss of a harmonic generator using an ideal nonlinear reactance is zero for any order of frequency multiplication. The maximum power transfer is a function of the order of multiplication and of the normalized nonlinearity coefficient which is generating the specific harmonic. The maximum power transfer for a specific nonlinear reactive element decreases with increasing order of the harmonic and also decreases for decreasing nonlinearity. In practical circuits one achieves the theoretical predicted high conversion efficiencies only for very low order multiplications for which the nonlinearity coefficient is relatively high. For higher order harmonics the matching problem gets increasingly more difficult and circuit efficiency decreases such that the overall conversion efficiency decreases fairly rapidly for higher order multiplication. /15/

In order to increase the conversion efficiency and the power transfer in practical generators the merits of using multiple conversion are to be investigated. In the normal operation of harmonic generators only two frequencies are present, the fundamental and the desired harmonic frequency. In a multiple conversion type of operation as shown in the example of a 3rd harmonic generator in Figure 2 below, other frequencies are also present and are terminated in "idler" circuits.

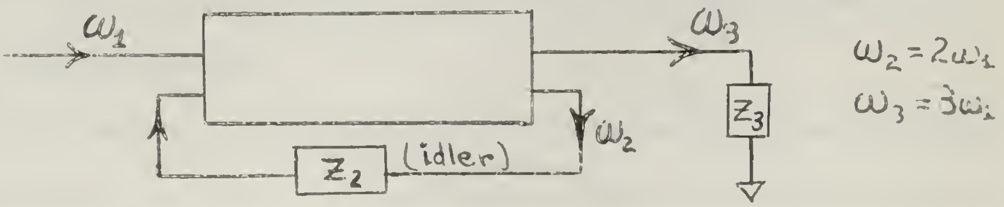

Figure 2

These idling frequencies can then be used for secondary harmonic generation and mixing processes in the same nonlinear element which will convert power into the wanted harmonic frequency. This can be thought of also as a type of positive power feedback where we are trying to reclaim power that has been converted into unwanted frequencies and use it to generate more power at our desired frequency, thus decreasing our conversion loss. If this could be done in the proper way, enhancement of the conversion efficiency and power transfer should be expected over that of the two frequency type generator, especially where the two frequency device is limited because of insufficient nonlinearity in the characteristic of the nonlinear element.

The nonlinear element available for this experiment was the basically square-law abrupt junction capacitive diode. This allows us to emphasize the principle of multiple conversion since the element delivers only 2nd harmonic without additional circuitry due to this second order nonlinearity. This also is a disadvantage because we cannot investigate the additional problem of great interest here -- that of the relative phasing that would be necessary between the direct conversion power and the multiple conversion mode power because the direct power is so very small for this nonlinear element.

The original investigation was commenced with the idea of showing that the multiple conversion process was practical and to try to obtain data on the effect of the loading of the "idler" circuit on the desired harmonic frequency output.

Since the harmonic generation process is an energy transfer problem, it was decided to look into the Hamiltonian method of analysis to obtain

a large signal theory that would be suitable for the problem and the circuit. The work on the theory was done by Dr. Peter Sturrock, Varian consultant, simultaneously with the experimental circuit building and testing done by this student. Both the theory and the experimentation as presented in this paper reached their conclusions at the same time.

The experimental device was built to be a microwave analog circuit operating at a fundamental frequency of 1 megacycle in order to obtain good data with available instruments, to make use of lump constant circuit elements, and to operate the nonlinear junction diode in a frequency well below its cut-off frequency.*

Another objective of this report that has become apparent while observing the multiple conversion process is that of the feasibility of using this process to get multiple frequency output by terminating the "idler" circuits in useful loads. A device of this type may have possible laboratory applications if not commercial.

---

* Cut-off frequency of V-33 Varicap is 100 MC.

Nonlinear Reactance Harmonic Generation Theory

a. General Discussion of Theory and Methods.

The theory of harmonic generation using nonlinear reactance elements has been well investigated for the two frequency case, that is, where the only frequencies are the fundamental and the desired harmonic. A relatively simple small signal theory for this case has been developed by Chang /12/ from his earlier work on parametric amplifiers. Leeson and Weinreb have developed a very complete large signal analysis for this two frequency case. /15/ In both of these analyses the coefficients of the nonlinear characteristic will be a limiting factor for higher order harmonic generation.

A large signal analysis of the multiple conversion process has been developed by Airborne Instruments Laboratories. This analysis is included in their reports on Air Force Project No. 4589. This theory is presented in Appendix I. The theory is developed for a very specific nonlinear element, the abrupt junction capcitance diode and could be done for each type nonlinear element. The theory can be applied to the experiment of this paper since this was the nonlinear element used. There are two difficulties with A. I. L.'s approach -- it is complex to work out, and it is for a specific nonlinear element case. Therefore there is still a need for a general theory for any nonlinearity where the energy transfer relationships are shown. It is for this reason that an investigation of the harmonic generator by Hamiltonian methods should be undertaken. This theory as developed by Dr. Peter Sturrock, Varian Associate's consultant, is presented in the following pages. A brief introduction to the Hamiltonian from reference 18 is given before this theory to aid the reader unfamiliar with Hamilton's Principle.

Brief Introduction to Hamilton's Principle [18]

The elementary formulation of the laws of mechanics is Newton's; it involves in an essential manner the basic concept of force. There are numerous other formulations based on different fundamental ideas, particularly the energy concept, which have been proposed throughout the history of the subject. The most important of which is Hamilton's principle. It should be regarded as a parallel fundamental postulate of mechanics which may be useful in cases where Newton's mechanics laws are cumbersome to apply.

Hamilton's principle takes for granted that one has a knowledge of the Energy -- both kinetic, T, and potential, V, -- of the system where T (kinetic energy) of the system is a function of the coordinates and their derivatives and where V (potential energy) of the system is a function of the coordinates and possibly time. From the functional form of T and V it then permits the deduction of coordinates of time.

Hamilton's principle postulates that the integral

$$\int_{t_1}^{t_2} (T - V) \, dt$$

shall have a stationary value. The integral, T - V, is called the Lagrangian function. We shall only consider conservative mechanical systems, that is, systems for which V is a function of the system coordinates only.

Now considering our system in generalized coordinates, $q_1, q_2, \ldots q_n$, where n is the number of degrees of freedom, V will be a function of the q's, but will not be a function of $\frac{dq}{dt}$. The kinetic energy T will be, however, a function of the q's as well as the $\frac{dq}{dt}$'s (except

when Cartesian coordinates are used.) The principle then states that

$$\int_{t_1}^{t_2} \left[T\left(q_1, q_2, \cdots q_n; \frac{dq_1}{dt}, \frac{dq_2}{dt}, \cdots \frac{dq_n}{dt}\right) - V(q_1, q_2, \cdots q_n) \right] dt = 0$$

Now apply this principle directly to an electrical circuit consisting of L and C. If q is the charge and $I = \frac{dq}{dt} = q_t$ (the current in a simple circuit which has capacitance C and self-inductance L) the total energy at any instant may be shown to be

$$\frac{1}{2} L \, q_{t_i}^{2} + \frac{1}{2} \frac{q_i^{2}}{C} \qquad (i=1, 2, \ldots n)$$

It is clear from the above and various mechanic-electrical analog methods /19/ that the first of these two terms may be regarded as kinetic energy T, and the second as the potential energy V -- provided the q's or charges are chosen as the generalized coordinates of the system. The intuitive meaning of T and V here become obscured as they do in many problems of advanced mechanics.

3(c)

Nonlinear Circuits Treated by Hamiltonian Methods /16/

In treating lossy nonlinear circuits, there is probably no substitute for Kirchhoff's equations as the point of departure. However, in discussing lossless (purely reactive) systems, it is possible to begin with a Lagrangian or Hamiltonian formulation. The second approach is attractive for exploratory work, since the Hamiltonian description is more economical and permits the use of such techniques as canonical transformations to bring out the particular aspects of the problem which are of most interest. For instance, in considering the design of a system to effect harmonic generation, the variables can be transformed is such a way that the rapid oscillatory variation is taken out of the problem by a canonical transformation and a judicious selection from the remaining terms. This leaves a much simpler statement of the problem which gives further insight into the system; moreover, equations from which the rapid variation has been removed would be a much lighter computational program than the solution of the original set of equations.

Consider the harmonic oscillator defined by the Hamiltonian

$$H = \frac{1}{2m}p^2 + \frac{1}{2}m\omega^2 q^2 \tag{1}$$

With a general solution of the form

$$\begin{aligned} q &= (2m\omega)^{-\frac{1}{2}}\left(b\,e^{j\omega t} + j b^{\dagger} e^{-j\omega t}\right) \\ p &= \left(\tfrac{1}{2}m\omega\right)^{\frac{1}{2}}\left(j b e^{j\omega t} + b^{\dagger} e^{-j\omega t}\right) \end{aligned} \tag{2}$$

which is complex and canonical.

$$b^{\dagger} = -jb^{*}$$

The variables b, and $b^{\dagger}$ are the constants of the motion.

Consider, as a simple example of a "parametric" circuit, the system shown in Figure 3. The appropriate dynamic variables q_1, q_2, q_3, represent "charge displacement" through the circuits indicated. We characterize the nonlinear capacitance by the stored energy U expressed as a function of charge q upon the plates. This may be expanded as follows

$$U(q) = \tfrac{1}{2}U'' q^2 + \frac{1}{6} U''' q^3 + \dots \tag{3}$$

if it is assumed that there is no linear term. The Hamiltonian for this system may be written as

$$H = H^0 + H^I \tag{4}$$

where H^0 contains the uncoupled circuit contributions

$$\begin{aligned} H^0 = {} & \frac{1}{2}\left(L_1^{-1} p_1^2 + C_1^{-1} q_1^2\right) \\ & + \frac{1}{2}\left(L_2^{-1} p_2^2 + C_2^{-1} q_2^2\right) \\ & + \frac{1}{2}\left(L_3^{-1} p_3^2 + C_3^{-1} q_3^2\right) \end{aligned} \tag{5}$$

which are of no interest in this part of the problem, and H^I contains the coupling and driving terms:

$$\begin{aligned} H^I = {} & -v_1(t) q_1 - v_2(t) q_2 - v_3(t) q_3 + \frac{1}{2} U''(q_1 + q_2 + q_3)^2 \\ & + \frac{1}{6} U'''(q_1 + q_2 + q_3)^3 + \dots \end{aligned} \tag{6}$$

If we now write

$$\omega_1^2 = 1/L_1 C_1 \quad \text{and} \quad \alpha_1 = \left(\frac{1}{4} L_1^{-1} C_1\right)^{1/4}, \text{etc.,} \tag{7}$$

the transformation equation 2 takes the form, for the Hamiltonian equation ,

$$q_1 = \alpha_1 \left(b_1 e^{j\omega_1 t} + j b_1^{\dagger} e^{-j\omega_1 t} \right), \text{etc.,} \tag{8}$$

It can be seen from equation 6 that, with this set of variables, the Hamiltonian for the complete system is given by

$$\begin{aligned} H^I = & -\alpha_1 v_1(t)(b_1 e^{j\omega_1 t} + j b_1^{\dagger} e^{-j\omega_1 t}) + \cdots + \cdots \\ & + \frac{1}{2} U'' \left[\alpha_1(b_1 e^{j\omega_1 t} + j b_1^{\dagger} e^{-j\omega_1 t}) + \cdots + \cdots\right]^2 \\ & + \frac{1}{6} U''' \left[\alpha_1(b_1 e^{j\omega_1 t} + j b_1^{\dagger} e^{-j\omega_1 t}) + \cdots + \cdots\right]^3 \end{aligned} \qquad (9)$$

Since $H^0 = 0$, the canonical equations reduce to

$$\dot{b}_1 = \frac{\partial H^I}{\partial b_1^{\dagger}} \quad , \quad \dot{b}_1^{\dagger} = -\frac{\partial H^I}{\partial b_1} \text{ , etc.,} \qquad (10)$$

So far no approximations have been made. We now indicate how it is possible to extract from this formalism an approximate set of equations valid for weak coupling between the circuits. Initially consider the case that

$$\omega_3 = \omega_1 + \omega_2 \qquad (11)$$

and that the driving terms V_1 (t) are expressible as

$$v_1(t) = V_1 e^{j\omega_1 t} + V_1^{*} e^{-j\omega_1 t} \text{ , etc.,} \qquad (12)$$

Then we may pick out from the Hamiltonian equation 9 the zero-frequency contribution:

$$\begin{aligned} H^I_{zf} = & -\alpha_1 (V_1^{*} b_1 + j V_1 b_1^{\dagger}) - \cdots - \cdots \\ & + U''(\alpha_1^2 b_1 b_1^{\dagger} + \cdots + \cdots) \\ & + U''' \alpha_1 \alpha_2 \alpha_3 (j b_1 b_2 b_3^{\dagger} - b_1^{\dagger} b_2^{\dagger} b_3) \\ & + \cdots \end{aligned}$$

[illegible]

$$[illegible]$$

$$[illegible]$$

$$[illegible]$$

[illegible]

$$[illegible]$$

[illegible]

$$[illegible]$$

[illegible]

$$[illegible]$$

[illegible]

From this formula is obtained the low-frequency contribution to the variation of the variables b_1, etc, and find b'_1, etc. from equation 10:

$$\dot{b}_1 = -j\alpha_1 V_1 + jU''\alpha_1^2 b_1 + jU'''\alpha_1\alpha_2\alpha_3 b_2^* b_3,$$

$$\dot{b}_2 = -j\alpha_2 V_2 + jU''\alpha_2^2 b_2 + jU'''\alpha_1\alpha_2\alpha_3 b_1^* b_3 \qquad (14)$$

$$\dot{b}_3 = -j\alpha_3 V_3 + jU''\alpha_3^2 b_3 + jU'''\alpha_1\alpha_2\alpha_3 b_1 b_2$$

The above set of equations involve the effect of the driving forces, of the frequency displacement due to the coupling capacitance, and of mode coupling due to the nonlinearity of the capacitance. The high-frequency variation has been removed completely from the dynamic variables.

If initially considering only the coupling terms involving U''' , it may be verified that this coupling satisfies the Manley-Rowe equations 11. The energy to be attributed to the modes is given by

$$E_1 = j\omega_1 b_1^\dagger b_1 = \omega_1 b_1^* b_1 \text{ , etc.,} \qquad (15)$$

from which it may be verified that

$$\frac{\dot{E}_1}{\omega_1} = \frac{\dot{E}_2}{\omega_2} = -\frac{\dot{E}_3}{\omega_3} \qquad (16)$$

The second terms, involving U'' (equation 14), give rise to frequency shifts of amount

$$\Delta\omega_1 = U''\alpha_1^2 \text{ , etc.,} \qquad (17)$$

The first terms of equation 14 involving V_1 etc., may represent the driving forces or the effect of a load. If the loads are characterized by complex impedances Z_1 , etc., it is found that V_1 , etc. are given by

$$V_1 = j\omega_1 Z_1 \alpha_1 b_1 \text{ , etc.,} \qquad (18)$$

Hence we may readily rewrite equations 14 for the case in which the third circuit is excited by a driving term, and the first and second circuits contain resistive loads.

The choice of equation 11 for the frequency relationship is appropriate to the discussion of parametric amplification. Let us now consider the relationship appropriate to harmonic generation:

$$\omega_1 = \omega , \quad \omega_2 = 2\omega , \quad \omega_3 = 3\omega , \text{etc.,} \tag{19}$$

Then the nonlinear term in U''' involves two important interactions associated with the frequency relations

$$\omega_2 = \omega_1 + \omega_1 , \quad \omega_3 = \omega_1 + \omega_2 \tag{20}$$

There is no difficulty in picking out the extra contribution to equation 13, which is found to be

$$\frac{1}{2} U''' \alpha_1^2 \alpha_2 \left(j\, b_1^2 b_2^\dagger - b_1^{\dagger 2} b_2 \right) \tag{21}$$

Hence equations 14 are replaced by

$$\begin{aligned} \dot{b}_1 &= -j\alpha_1 V_1 + jU''\alpha_1^2 b_1 + jU'''\alpha_1^2\alpha_2 b_1^* b_2 + jU'''\alpha_1\alpha_2\alpha_3 b_2^* b_3 \\ \dot{b}_2 &= -j\alpha_2 V_2 + jU''\alpha_2^2 b_2 + j\tfrac{1}{2}U'''\alpha_1^2\alpha_2 b_1^2 + jU'''\alpha_1\alpha_2\alpha_3 b_1^* b_3 \\ \dot{b}_3 &= -j\alpha_3 V_3 + jU''\alpha_3^2 b_3 + jU'''\alpha_1\alpha_2\alpha_3 b_1 b_2 \end{aligned} \tag{22}$$

It would be interesting to compare the results of the above approximate equations for this simple case with computations which have already been made. In this example, V_1 represents a driving term, $V_2 = 0$, and V_3 is of the form of equation 18, representing a resistive load.

One may set up two relations of the form of equation 16, one for each of the interaction terms characterized by the frequency relations equation 20. Hence an 'energy-flow' chart as shown in Figure 4 may be

drawn up in which is adopted the convention that a square denotes a 'mode' of 'oscillator', a circle denotes a coupling mechanism, and a diamond denotes a source or sink of energy. The power flowing along each link is shown. It is seen that, according to the present model, all the power injected at frequency ω_1 is converted to frequency $3\omega_1$. However, the rate of conversion must be obtained by solving the equations 22 although it may be possible to extract general rules concerning the rate of conversion by further application of the action-transfer and frequency-shift relations.

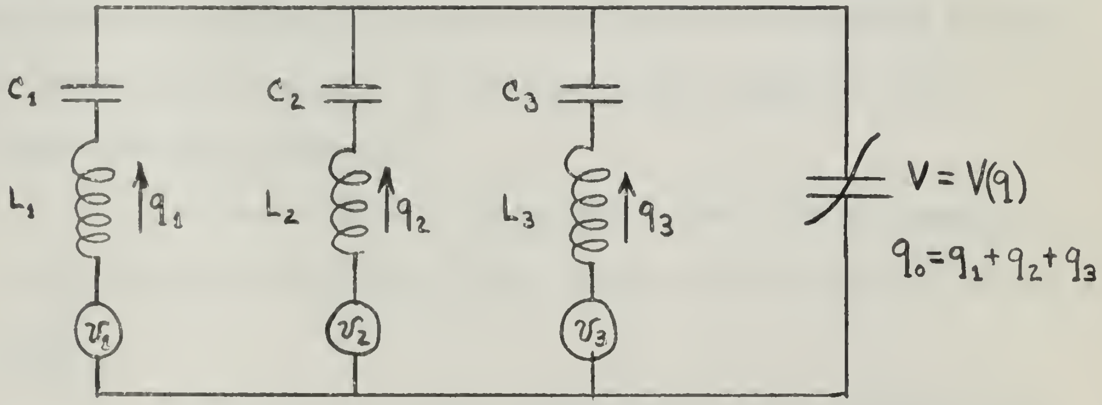

Parametric Circuit

Figure 3

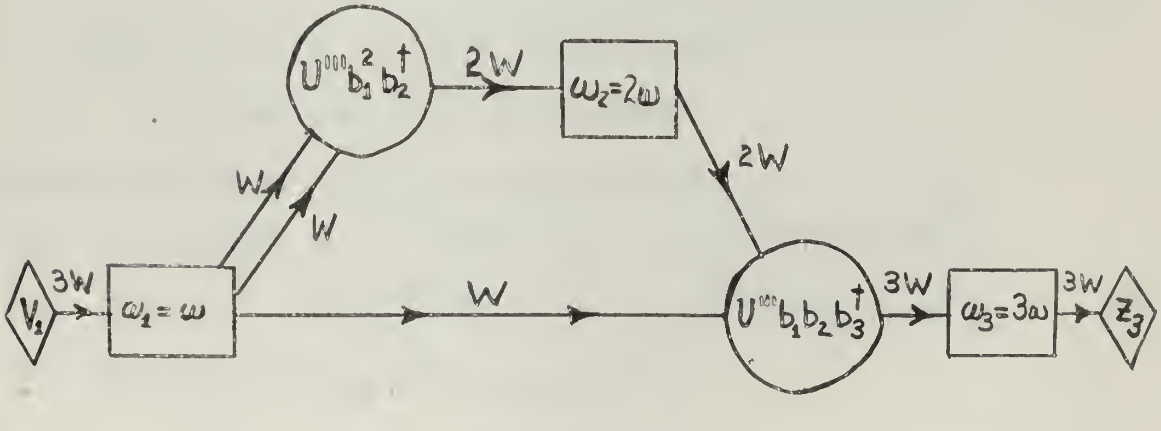

Energy Flow Chart

Figure 4

[illegible]

[illegible]

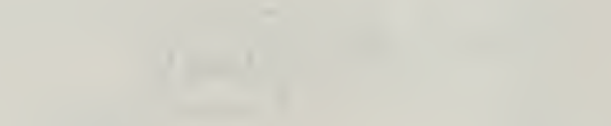

[illegible]

3(d)

A Solution to the Hamiltonian for the Multiple Conversion Process

The solution of the equations 22, as it stands, is quite difficult. If we look at the experimental circuit in which we are going to investigate this case where the 2nd harmonic power, P_2, is zero (assumed lossless) -- that is the 2nd harmonic circuit is a short circuit; we can eliminate the driving force or load term in the second equation of 22. If we maintain the driving force on the diode constant -- that is, the voltage across the diode, V_1, at the fundamental frequency -- the detuning terms involving U'' of equations 22 may be disregarded because we are effectively retuning. We now have a much simplified form.

These are the assumptions.

1. The three circuits (fundamental, 2nd, and 3rd harmonic frequencies) are decoupled except through the nonlinearity of the diode.

2. The effective or mean capacitance of the diode has been taken into account in determining the resonant frequencies of each of the three circuits.

3. We have assumed that there is an injected V_1 at $\;_1$ and only one load Z_3 $(Z_2 = 0)$, which is real.

4. Operation is at steady state.

Equation set 22 now takes the following form

$$\begin{aligned}
&\text{(a)} \quad 0 = -j\alpha_1 V_1 + jU'''\alpha_1^2 b_1^* b_2 + jU'''\alpha_1\alpha_2\alpha_3 b_2^* b_3 \\
&\text{(b)} \quad 0 = \qquad\qquad + \tfrac{1}{2} jU'''\alpha_1^2\alpha_2 b_1^2 + jU'''\alpha_1\alpha_2\alpha_3 b_1^* b_3 \qquad (23) \\
&\text{(c)} \quad 0 = -j\alpha_3 V_3 + jU'''\alpha_1\alpha_2\alpha_3 b_1 b_2
\end{aligned}$$

now the current equations are

$$(a)\quad i_1 = j\omega_1\alpha_1 b_1$$

$$(b)\quad i_2 = j\omega_2\alpha_2 b_2 \quad = j\,2\omega_1\alpha_2 b_2 \tag{24}$$

$$(c)\quad i_3 = j\omega_3\alpha_3 b_3 \quad = j\,3\omega_1\alpha_3 b_3$$

and the voltages present are

$$V_1 = -\widetilde{Z}_1 i \qquad \text{and} \qquad V_3 = Z_3 i_3$$

where $\widetilde{Z}_1$ is the input impedance.

Solving equations 23(b) and (c) for b_2 and b_3 in terms of b_1 we get:

$$b_3 = -\frac{1}{2}\,\frac{\alpha_1}{\alpha_3}\,\frac{b_1^2}{b_1^*} \tag{25}$$

$$b_2 = -j\frac{3}{2}\,\frac{\omega_1 Z_3}{\alpha_2 U''}\left(\frac{b_1}{b_1^*}\right) \tag{26}$$

now substituting b_3 and b_2 in equation 23(a) gives b_1 in terms of V_1 and Z_3.

$$b_1 = j\frac{4}{9}\,\frac{V_1}{\alpha_1\omega_1 Z_3} \tag{27}$$

Therefore we may solve for b_2 and b_3 by substituting equation 26 in equations 24 and 25.

$$b_2 = j\frac{3}{2}\,\frac{\omega_1 Z_3}{\alpha_1 U'''}\left(\frac{V_1}{V_1^*}\right) \tag{28}$$

$$b_3 = -j\frac{2}{9}\,\frac{1}{\alpha_3\omega_1 Z_3}\left(\frac{V_1^2}{V_1^*}\right) \tag{29}$$

These b's may now be put into current equation set 24 from which some very interesting results follow

$$i_1 = -\frac{4}{9}\,\frac{V_1}{Z_3} \tag{30}$$

$$i_2 = -\frac{3\omega_1^2 Z_3}{U'''}\left(\frac{V_1}{V_1^*}\right) \tag{31}$$

$$i_3 = \frac{2}{3}\,\frac{1}{Z_3}\left(\frac{V_1^2}{V_1^*}\right) \tag{32}$$

Equation 30 becomes

$$Z_3 = \frac{4}{9}\widetilde{Z}_1 \tag{33}$$

which says that in the lossless case using a nonlinear reactive element

in a multiple conversion process that the impedance reflected from the 3rd harmonic circuit into the fundamental circuit is a constant ration. From this idea of the reflection of impedance through the nonlinear element we can see the added importance of providing an impedance match at the input of the device. It is necessary to provide this matching to get the desired impedance reflection ratio through the nonlinear element. This may be thought of as a boundary value problem where one of the boundaries is that $\widetilde{Z}_1 = \frac{9}{4} Z_3$.

It is important to note that the diode characteristics do not affect the impedance ratio.

In equation 31 it is seen that the idler current i_2 is a function of the 3rd harmonic load and of the diode characteristic.

In equation 32 the output current i_3 is a function of the fundamental drive voltage and the 3rd harmonic load impedance.

The power flow into the device

$$P_1 = -\left(i_1^* V_1 + i_1 V_1^*\right) = \frac{8}{9}\frac{|V_1|^2}{Z_3} \tag{34}$$

using V_1 (rms)

$$P_1 = \frac{4}{9}\frac{|V_1|^2_{rms}}{Z_3}$$

Applying the Manley-Rowe conditions for the lossless case then

$P_1 = P_3$

Since V_1 has limits fixed by the diode characteristics it is observed that if Z_3 is decreased to zero in equation 34, maximum power would be delivered. However, this makes $Z_1 = 0$ also from equation 33, and we know that if this is the case no power is developed. Therefore there is some optimum Z_3, or stated in another way, there is some optimum

V_1 which is a function of Z_3. To solve for V_1 in terms of Z_3 take equations 30, 31, and 32

$$i_1 = -\frac{4}{9}\frac{V_1}{Z_3} \qquad = j\omega_1 q_1{}^1$$

$$i_2 = -3\frac{\omega_1^2 Z_3}{U'''}\frac{V_1}{V_1^*} = j\omega_2 q_2 = j2\omega_1 q_2$$

$$i_3 = -\frac{2}{3}\frac{1}{Z_3}\frac{V_1^2}{V_1^*} = j\omega_3 q_3 = j3\omega_1 q_3$$

solving for the q's

$$q_1 = +j\frac{4}{9}\frac{V_1}{Z_3\omega_1} \tag{35}$$

$$q_2 = +j\frac{3}{2}\frac{\omega_1 Z_3}{U'''}\left(\frac{V_1}{V_1^*}\right) \tag{36}$$

$$q_3 = +j\frac{2}{9}\frac{1}{Z_3\omega_1}\left(\frac{V_1^2}{V_1^*}\right) \tag{37}$$

and

$$|q_1| + |q_2| + |q_3| = \frac{1}{2}Q_{total} \tag{38}$$

because the q's are complex. Now substituting 35, 36, and 37 in equation 38 and solving for V_1

$$|V_1| = \frac{3}{4}\left(Q\omega_1 Z_3 - \frac{3\omega_1^2 Z_3^2}{U'''}\right) \tag{39}$$

now maximizing V_1 in respect to Z_3

$$\frac{d|V_1|}{dZ_3} = \frac{3}{4}Q\omega_1 - \frac{9}{2}\frac{\omega_1^2 Z_3}{U'''} = 0 \tag{40}$$

$$Z_3 = \frac{1}{6}\frac{QU'''}{\omega_1}$$

[1] from equation 8 and $i = \frac{dq}{dt}$

Substituting this back in 39 we get the optimum V_1

$$V_1 = \frac{1}{16} Q U''' \tag{41}$$

Now substituting equations 40 and 41 into the power equation 34 we get the "optimum" power transfer equation

$$P_{1\,opt} = \frac{1}{48} \omega_1 Q^3 U''' \tag{42}$$

By optimizing V_1 and using suitable diode bias we are driving the nonlinear element on the most ideal portion of its nonlinearity -- that is, where the desired nonlinearity coefficients are greatest for this conversion process.

Now since V_1 and V_{bias} were kept fixed in the experiment we cannot optimize in the above method, but we can use equation 39 in equation 34 and maximize P_1 with respect to Z_3 which for this experiment should determine the maximum power transfer. Substituting equation 39 into the power equation 34 then

$$P_1 = \frac{1}{2}\left(Q^2 \omega_1 Z_3 - \frac{6 Q \omega_1^3 Z_3^2}{U'''} + \frac{9 \omega_1^4 Z_3^3}{U'''^2}\right) \tag{43}$$

and taking $\frac{dP_1}{dZ} = 0$ to get the maximum power transferred we get

$$Z_3 = \frac{1}{3} \frac{Q U'''}{\omega_1} \ ; \ \frac{1}{9} \frac{Q U'''}{\omega_1}$$

now putting these values of Z_3 back into equation 43 we have

for $Z_3 = \frac{1}{3} \frac{Q U'''}{\omega_1}$ $P_1 = 0$

for $Z_3 = \frac{1}{9} \frac{Q U}{\omega_1}$ (44)

$P_{1max} = \frac{2}{81} \omega_1 Q^3 U'''$

Therefore it is seen that the maximum power transferred for this case -- where V_1 is a constant -- is a function of frequency and the energy stored in the nonlinear reactance. Energy is transferred at

the rate of 0.155 units per cycle of the fundamental frequency.

Appendix III gives a development of the Energy vs Charge characteristics of the nonlinear element used in the experiment circuit from which values of Q and U''' can be obtained.

Experimental Circuit Design

The basic circuit used stems directly from the Manley-Rowe circuit, Figure 1, and from Airborne Instruments Laboratorie's second harmonic generator, equation 14. In the Manley-Rowe circuit there is no coupling between the various frequency branches except through the nonlinear reactance element. Ideal filters prevent the flow of the harmonic frequencies except in their assigned branches. To have a maximum real power transfer in each frequency branch we must have a reactance in each frequency branch of equal and opposite sign to be resonant with the mean or effective reactance of the nonlinear reactive element.

The circuit shown in Figure 5 was developed to meet the above criteria. The device as it was constructed is shown in the photograph Figure 6. Starting with the measured data on the nonlinear capacitance junction diodes available as listed in Appendix II, a value of effective capacitance, C_{eff}, was obtained for 8 V-33 Varicaps and 1 V-20. The following equations used to determine C_{eff} yield similar results./13,15/

(a)
$$\frac{1}{C_{eff}} = \frac{1}{2}\left(\frac{1}{C_2} + \frac{1}{C_1}\right)$$

C_1 and C_2 are the extreme values of capacitance from just before forward conduction to reverse breakdown of the diode, that is the working range of the diode.

or

(b)
$$C_o = \frac{C_1}{V_o^{\gamma}}$$

C_o = Capacitance at voltage bias V_o

V_o = Voltage bias

C_1 = Capacitance at terminal voltage V plus contact potential equal to 1 volt

γ = Exponent associated with the V vs C nonlinearity of the junction(from Appendix II)

Computation of C_{eff} using the above equations is found in Appendix IV.

After the value of effective capacitance was obtained for the selected bias point, inductances L_1, L_2, and L_3 were selected to resonate at the fundamental, 2nd, and 3rd harmonic frequencies which are 1, 2, and 3MC respectively.

To remove any input distortion and to provide complete 2nd and 3rd harmonic frequency loops, low impedance series resonance trap circuits, L_A, and C_A and L_B, C_b, are provided at point A. (Figure IV-1) At the output of the diodes, point B, another trap circuit was added to provide a low impedance path, L_{C1}, L_{C2}, and C_{C3}, for the fundamental current to prevent it from flowing in the 2nd and 3rd harmonic circuits

In the 3rd harmonic output loop a band-pass image type filter was used. (L_{3A}, C_{3A}, L_{3B}, C_{3B}) It was found that the impedance of this filter was not large enough at the 2nd harmonic frequency to prevent this component from flowing in the 3rd harmonic circuit so it was necessary to add a parallel tank circuit resonant at the 2nd harmonic frequency in series L_{3C}, C_{3C}.

To provide a high impedance to 3rd harmonic in the 2nd harmonic circuit a parallel tank circuit was added, L_{2A} and C_{2A}, to act as a filter or blocking element.

In the fundamental trap circuit it was also necessary to increase the impedance at 2nd harmonic and 3rd harmonic frequencies. Therefore parallel tank circuits resonant at these frequencies were added.

To maintain the bias level on the diode and to prevent a low impedence RF path in the output circuitry; a large resistor, R_{B2}, or a RF choke was needed.

To insure maximum energy transfer from a fundamental or driving source a high degree of matching should be used. Since the power source was abundant and we were not investigating this matching problem, a matched input was not used.

A discussion of circuit problems, the matching problem, and circuit alignment, will be found in Appendix IV.

After aligning the circuit as outlined in Appendix IV-B the following measurements were conducted.

a. Direct Conversion

As a 3rd harmonic generator without the 2nd harmonic circuit, input power at the fundamental frequency and output power at the 3rd harmonic frequency vs various values of R_{3L} were measured.

As a 2nd harmonic generator without the 3rd harmonic circuit included, measurements of power input and power output vs R_{2L} were made. Also measurements of power input and power output as the driving voltage on the diode at the fundamental frequency was changed for various R_{2L} were made.

b. Multiple Conversion

As a 3rd harmonic generator with the 2nd harmonic circuit included, input power at the fundamental frequency and output power at the 3rd harmonic vs R_{3L} with R_{2L} varied from 0 to 10 Kohms for each setting of R_{3L} were measured.

As a 3rd harmonic generator with the 2nd harmonic circuit included and $R_{2L} = 0$, measurements were made of power input and power output for various values of R_{3L} as the driving voltage on the diode at the fundamental frequency was changed.

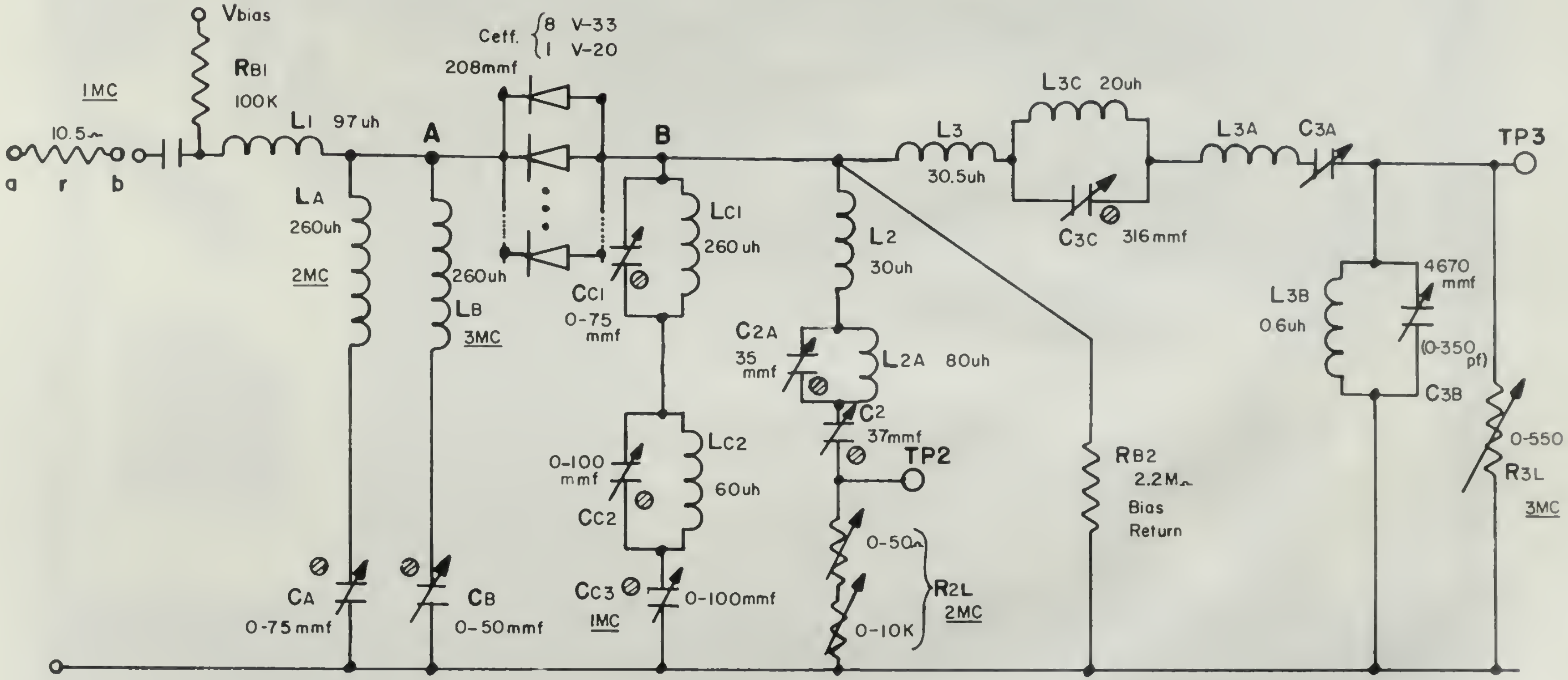

2nd & 3rd HARMONIC GENERATOR CIRCUIT

Figure 5

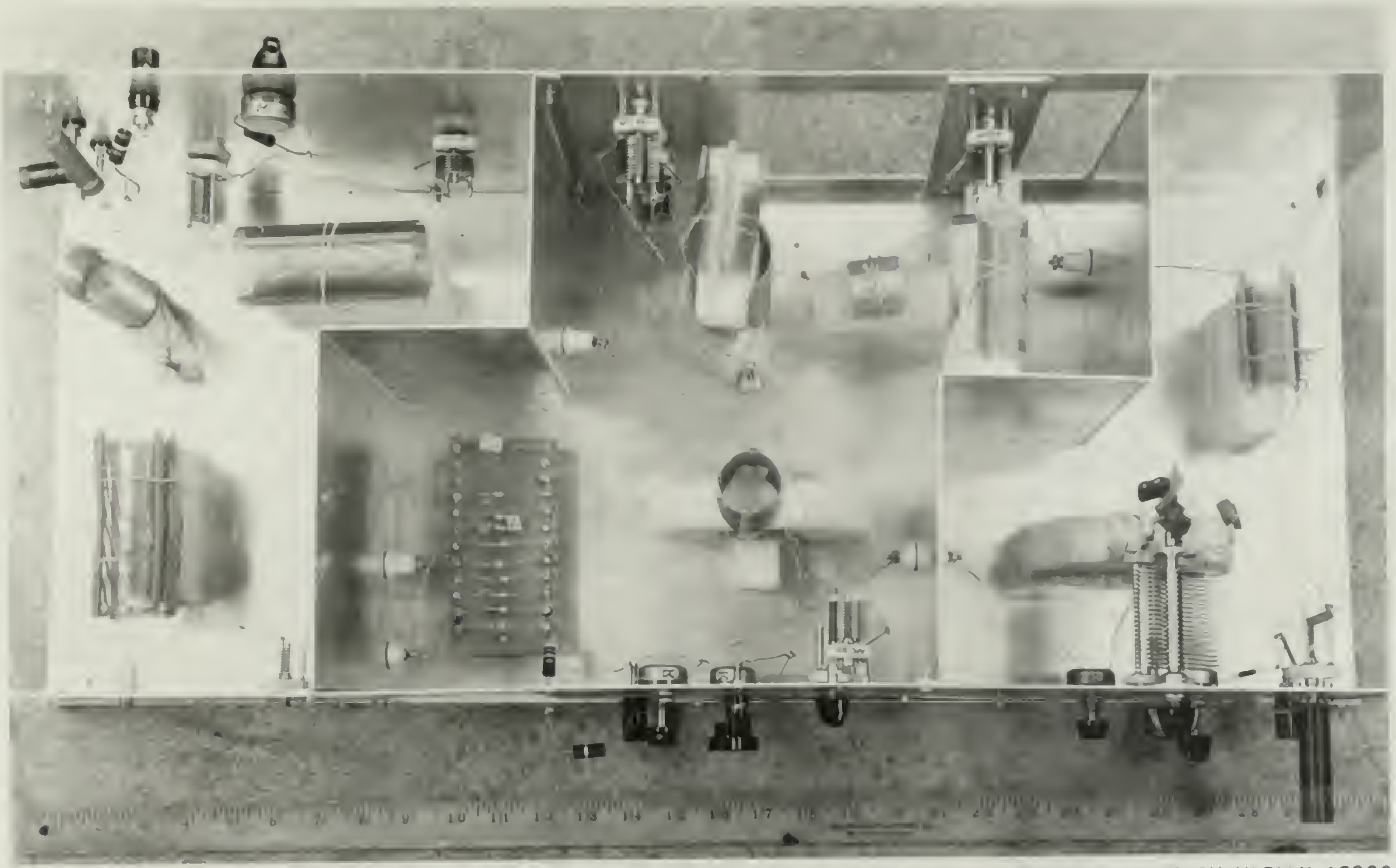

PHOTO COURTESY VARIAN ASSOC.

HARMONIC GENERATOR (1 TO 3MC)

FIGURE 6

5

Experimental Results and Conclusions

A. Direct conversion process

1. 3rd harmonic generation

The 2nd harmonic circuit was disconnected. Measurements of input and output power were made while varying R_{3L} with V_1 (voltage across diode at the fundamental frequency) held constant. The data from this part of the experiment is plotted in Figure 7 below.

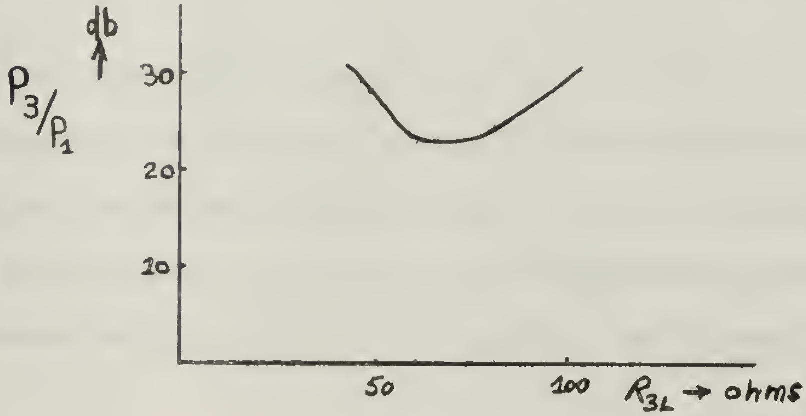

Figure 7

Only enough data was taken here to show the general range of conversion efficiencies. The best operating conditions achieved are as follows:

Fundamental input power, P_1 (1MC)	1.5 mw
3rd harmonic output power, P_3 (3MC)	6.5 μw
Conversion loss P_3/P_1	23 db
R_{3L}	60 ohms

2. 2nd harmonic generation

When operated as a 2nd harmonic generator the 3rd harmonic output circuit was disconnected. Two curves are shown below plotted from the data taken. Figure 8 is a plot of conversion efficiency vs various values of R_{2L}. Figure 9 is a plot of conversion efficiency vs V_1 for various values of R_{2L}.

[illegible]

[illegible]

[illegible]

[illegible]

[illegible]

[illegible]

[illegible]

The best operating conditions achieved for the 2nd harmonic generator are as follows:

Fundamental input power, P_1, (1MC)	7.67 mw
2nd harmonic output power, P_2, (2MC)	5.52 mw
Conversion loss, P_2/P_1	1.4 db
Bias voltage	-10 vdc
V_1 across diode	7.07 v
R_{2L}	150 ohms

From these above results we can conclude that as a direct conversion or two frequency device, the experimental circuit is an efficient 2nd harmonic generator and a very poor 3rd harmonic generator. This is as should be expected from the predominantly second order nonlinear characteristic of the abrupt junction capacitance diode.

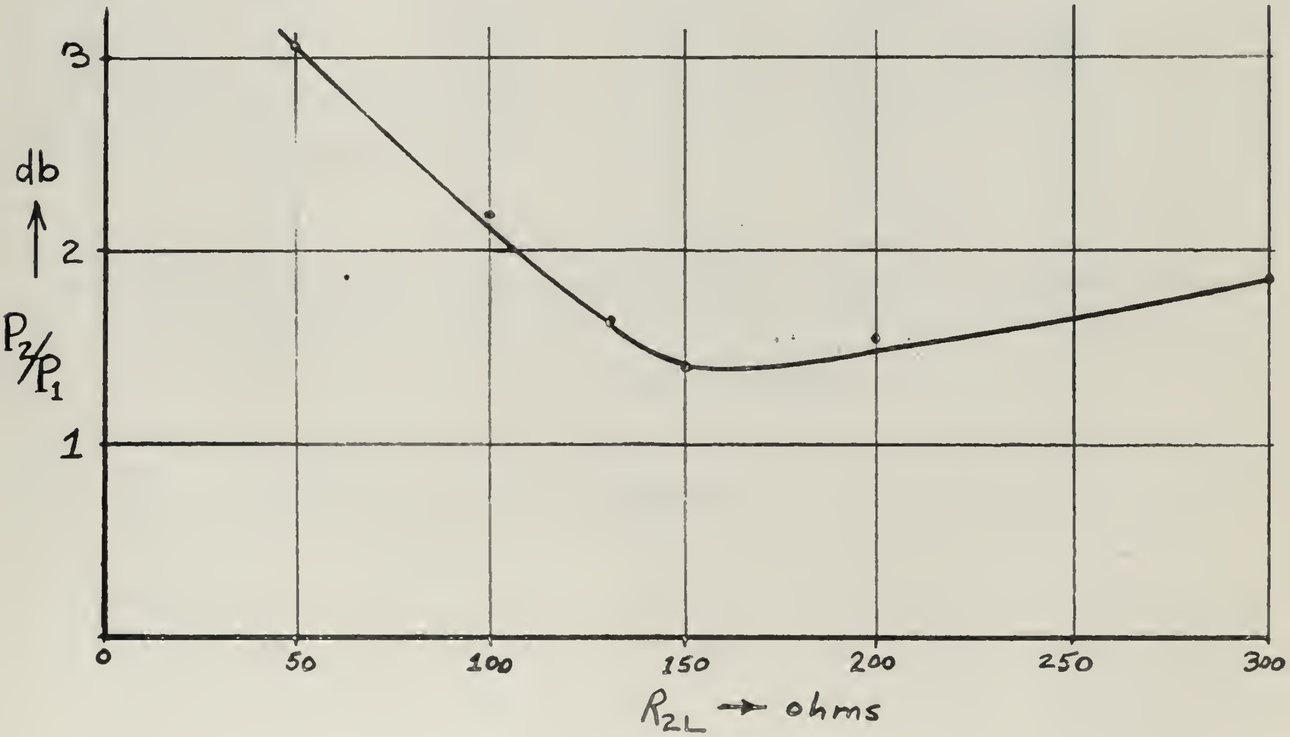

Figure 8

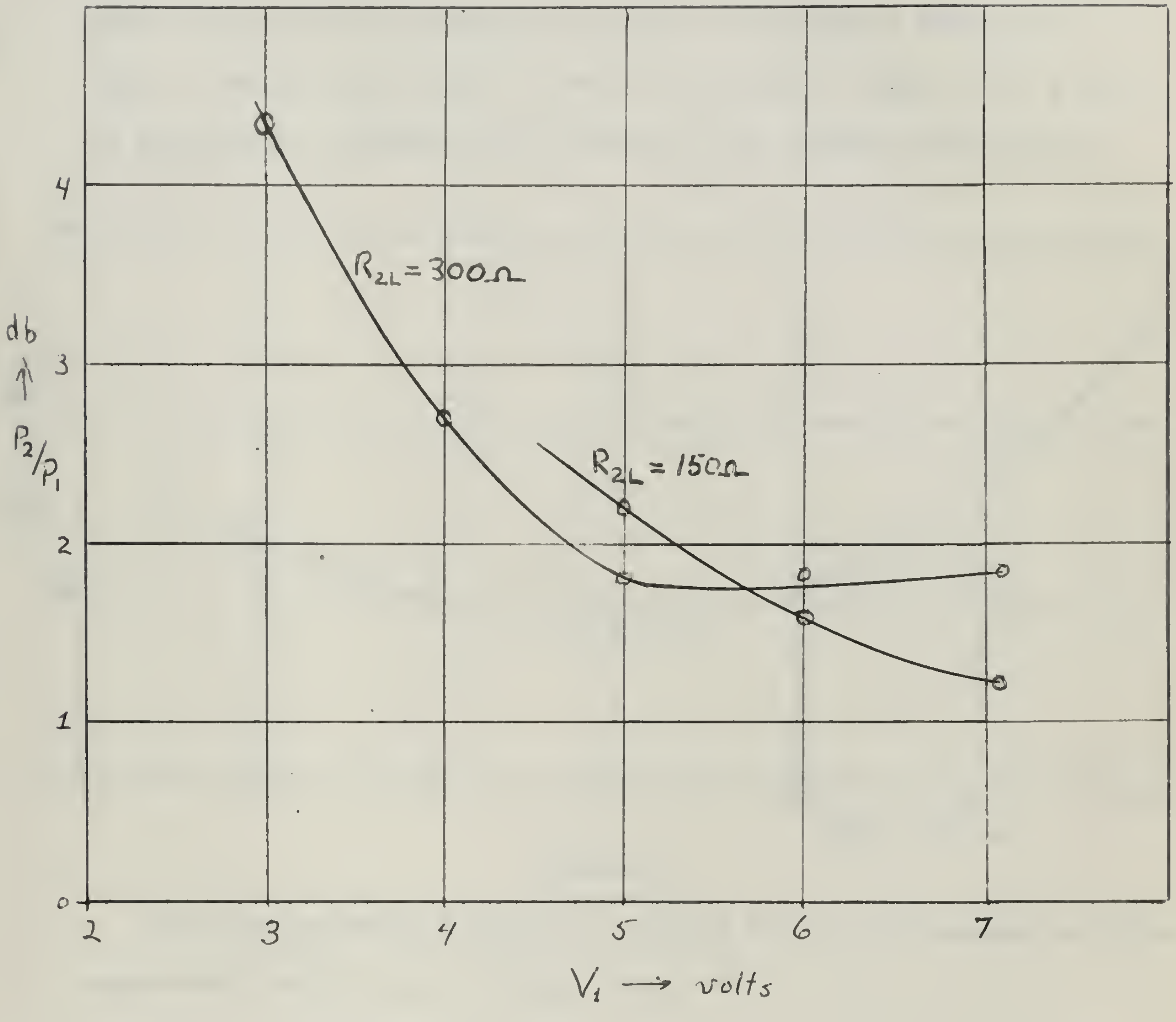

Figure 9

5(b)

Multiple Conversion Process

The device was operated as a 3rd harmonic generator with the 2nd harmonic output circuit connected. Data taken is plotted in the two curves shown below. Figure 10 is a plot of conversion efficiency, P_3/P_1 , versus R_{3L} . $R_{2L} = 0$ and V_1 = constant. Figure 11 is a plot of conversion efficiency P_3/P_1 versus V_1 for various values of R_{3L}.

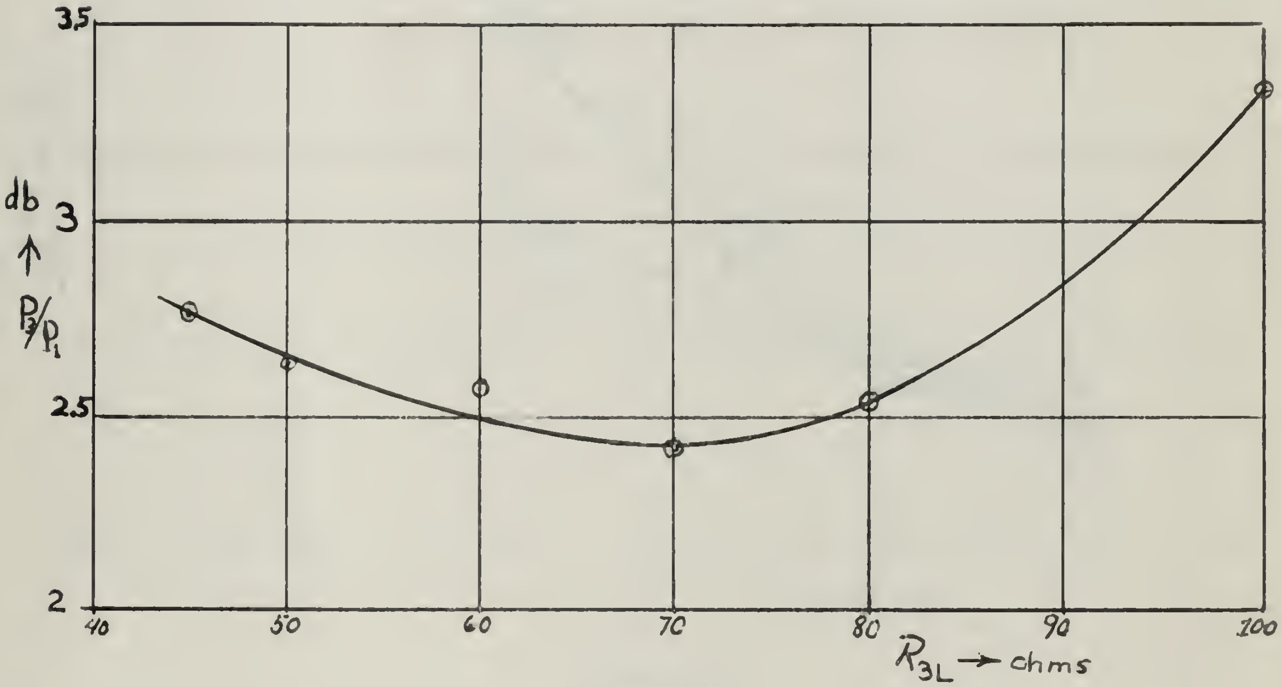

Figure 10

The best operating conditions achieved for the 3rd harmonic multiple conversion process are as follows. ($R_{2L} = 0$)

Fundamental input power P_1 (1 MC)	13.5 mw
3rd harmonic output power P_3(3 MC)	7.71 mw
Conversion loss (P_3/P_1)	2.42 db
Bias voltage	- 10 dc
V_1 (across diode at fundamental frequency)	7.07 v
R_{3L}	70 ohms
R_{in}	124 ohms

[illegible]

[illegible]

[illegible]

[illegible]

From Appendix IV the optimum R_{3L} calculated was 61 ohms. This shows fairly good correlation with the experimental results obtained above.

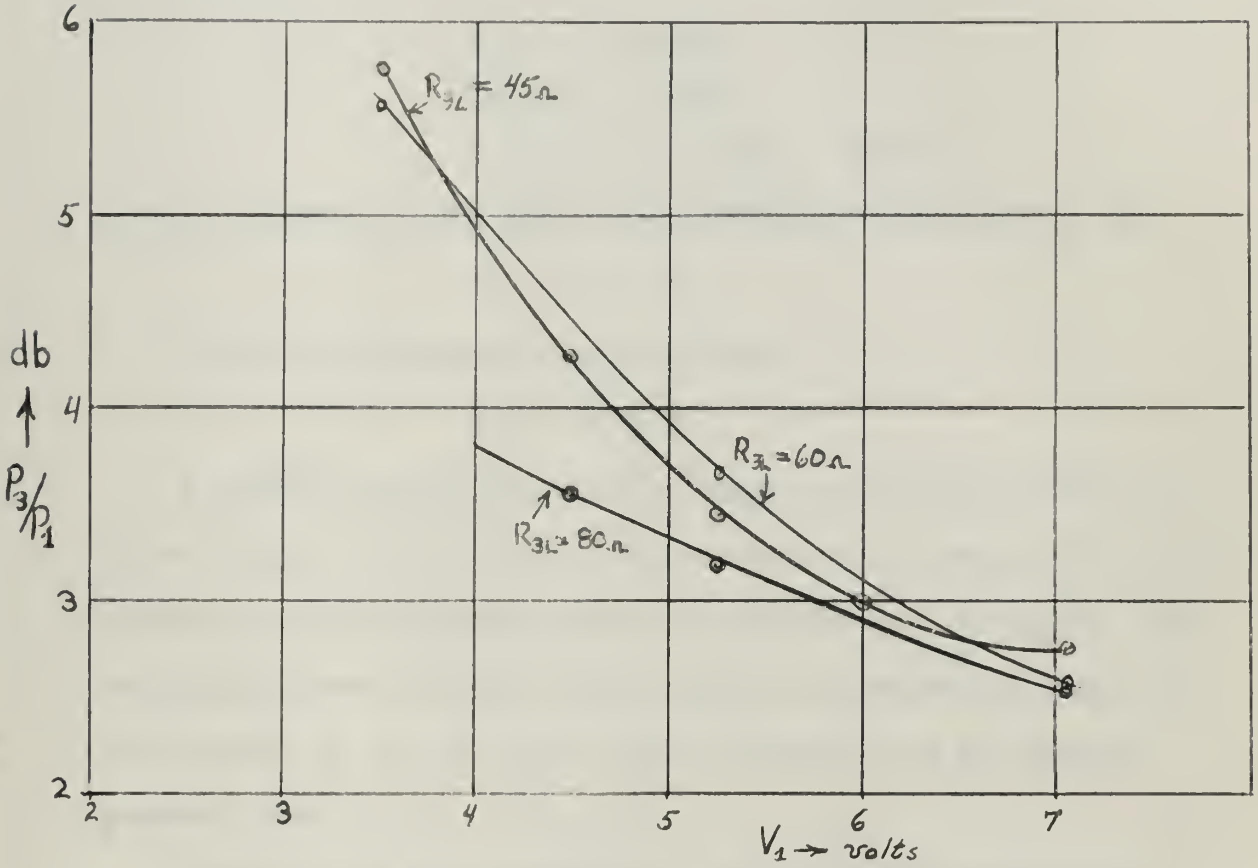

Figure 11

From Figure 11 it is observed that $V_1 = 7.07$ v gives the best conversion efficiency in this circuit as constructed.

It is concluded from this experimentation that the multiple conversion process is an effective method for harmonic generation.

The following disucssion is provided to show correlation of the experimental results and the theory of section 3.

$R_{in} = R_1 \text{ loss} + R_1$

$R_1 \text{ loss} = 24$ ohms

$R_1 = 124 - 24 = 100$ ohms

R_1 is the value of resistance reflected from the load R_{3L} and

and the losses of the output circuit through the nonlinearity -- assuming idling losses are zero. Since the diode doesn't know a loss from a load we can lump R_{3L} and the loss resistance, R_3 loss, together to form R_3.

$$R_{3L} = 70 \text{ ohms}$$

$$R_3 \text{ loss} = 19 \text{ ohms}$$

$$R_3 = 70 + 19 \text{ ohms} = 89 \text{ ohms}$$

From the solution to the Hamiltonian analysis we get equation 32

$$R_3 = 4/9 \ R_1$$

From the experimental results we have

$$R_3 = 0.89 \ R_1 \ .$$

A possible explanation for this result is that since there is a finite loss in the 2nd harmonic circuit we are not getting the reflected impedence multiplying effect that is indicated from the theory. The explanation seems plausible when we note the discussion on page C-3 of reference 14 for the large signal analysis for a 2nd harmonic generator where R_1 in $= R_2$ out.

From Appendix I and Appendix IV, the calculated optimum R_{3L} is 61 ohms. The experimental results give R_{3L} = 89 ohms if we include losses which is fairly good correspondence.

Using equation 43 and solving for the maximum Power transfer

$$P_1 = \frac{2}{81} \omega_1 Q^3 U''' \qquad \omega_1 = 2\pi \times 10^6$$

$$U''' = 1,877 \times 10^{17}$$

$$= 5.58 \text{ mw} \qquad Q = 5.76 \times 10^{-9}$$

U''' and Q from App. II

$P_{1 \text{ in}}$ measured was 13.5 mw

$P_{3 \text{ out}}$ measured was 7.7 mw

The P_1 calculated above is the power converted which corresponds fairly-well with the power $P_{3\ out}$. The P_{in} includes all power lost in the device. Thus we see correlation of the theory with the experiment.

5(c)

Effect of Idling Circuit Terminations

The idling circuit resistive termination, R_{2L}, was varied from 0 to 10 Kohms to observe the effects on the output power and on the conversion loss. Sufficient data was not taken to plot a good curve, but the general trend is noted in Figures 12 and 13 below. With $R_{2L} = 0$ there are still 19 ohms of resistive loss in the 2nd harmonic circuit and this is our zero point.

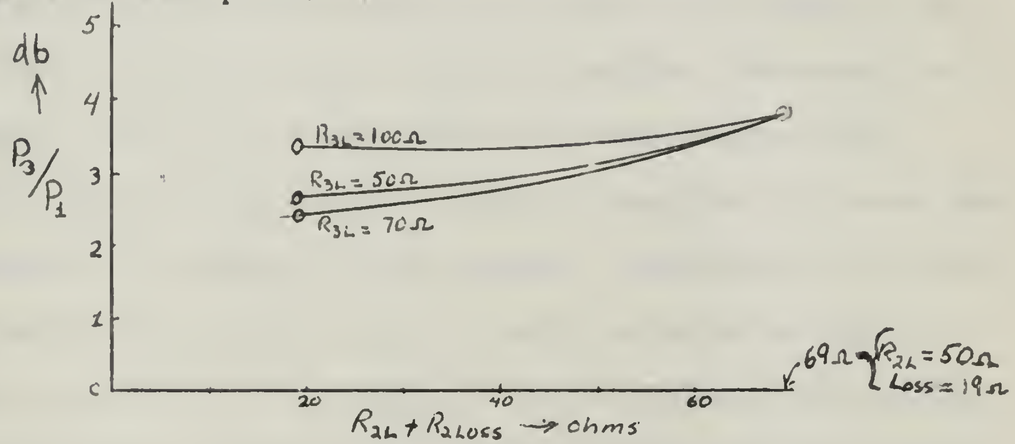

Figure 12

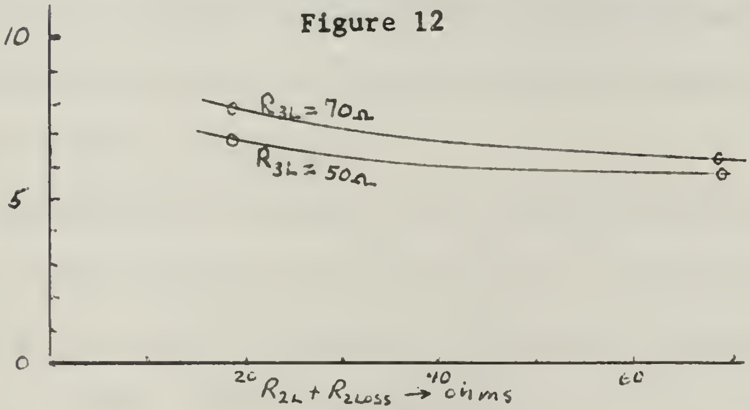

Figure 13

It was observed that as soon as any load, R_{2L}, was added P_3 began to drop off and the conversion loss began to increase. Input power remained about the same for R_{2L} small.

The large resistance, R_{2L} = 10 Kohms, had the same effect as disconnecting or open-circuiting the idling 2nd harmonic circuit. The

[illegible]

[illegible]

[illegible]

$$[illegible]$$

$$[illegible]$$

[illegible]

[illegible]

3rd harmonic output power was reduced to a very low value with a conversion loss of about 24 db.

A large reactance load was put in to the idling circuit in the form of a parallel tank circuit tuned close to the 2nd harmonic frequency. This had the same effect as a large resistive load -- that of presenting an open-circuit to the idling current.

From these results it is concluded that for efficient multiple conversion where direct conversion is very small, the losses in the idling circuit should be kept as small as possible. The method of resonating L_2 with C_{eff} of the diode at the optimum bias point maximizes the 2nd harmonic current which is being fed back to mix with the fundamental to produce the 3rd harmonic. Therefore for this case where the direct conversion output is small and we do not have to consider the addition of the phases of direct conversion and multiple conversion output, the termination of the nonlinear element should be an equal and opposite reactance determined from the mean value of the element, in this case, C_{eff}.

While determining the effects of the various values of idling load, R_{2L}, on the multiple conversion circuit; it was observed that the P_2 and P_3 were both of reasonable amplitude for values of R_{2L} up to about 100 ohms. Further data was taken and it was noted that for R_{2L} = 50 ohms, the total harmonic power converted, $P_2 + P_3$, is about the same amplitude as P_3 for $R_{2L} = 0$.

An example of these results follows:

R_{3L}	70 ohms
R_{2L}	50 ohms
3rd harmonic output power, P_3, (3MC)	6.23 mw
2nd harmonic output power, P_2, (2MC)	2.45 mw
Fundamental input power, P_1., (1MC)	15 mw

This data can be compared to our optimum operating condition on page 33.

Conclusively, this shows that a multiple frequency output device is possible. One application of such a device would be a microwave signal generator where reasonable input power at say 3 KMC could give reasonable outputs at 6, 9, and 12 KMC. At these frequencies calibrated variable cavities could be used to accomplish variable frequency output. The analysis of such a device will be very complex. The idea poses many interesting problems and is believed to be a practical one.

5(d)

Discussion of Losses

The problem of losses in the multiple conversion circuit is somewhat more complex than that of the two frequency device. /15/ There are still only two sources of loss: (1) the resistive losses of the nonlinear element and the associated filters for the fundamental, idling, and output circuits; and (2) the losses produced at unwanted frequencies in the source and the load.

The second source of loss caused by unwanted frequency dissipation should be made negligible by the use of realizable filters. If it cannot be, the approximation method of reference 15 is applicable.

The first source of loss is not as easily discussed. Idling circuit losses are reflected into the equivalent input resistance R_1 in the same manner as the output circuit losses and loads. The loss of the nonlinear element is present in all circuits and therefore has a larger effect than in the two frequency case. The simple method of reference 15 could be used in this case if R_1 could be effectively determined.

As a first approximation for estimating the efficiency of this type of device with idler circuit losses, combine the idler losses with losses in the output circuit and use the method shown in reference 15. This approximation will hold generally if idler losses are small and of about the same order of magnitude or less than output circuit losses.

R_a, R_b, and R_c are circuit losses

R_D is loss in diode

$i_{1\,in} = 10.5$ ma

$i_{3out} = 9.7$ ma

$P_{loss} = (10.5)^2\ 24 = 2.5$ mw

Fundamental

$P_{loss} = (9.7)^2\ (19) = 1.8$ mw

output

From Equation 30 section 3d

$$i_2 = \frac{3\omega_1^2 Z_3}{U'''} = \frac{3 \times 10^{12}(70)}{1.877 \times 10^{17}} = 11.2 \text{ ma}$$

U''' from Appendix III

$$P_{\substack{loss\\idler}} = (19)(11.2)^2 = 2.38 \text{ mw}$$

$$\text{Total losses} = \begin{aligned} &P_F + P_O + P_I = 6.66 \text{ mw (calculated)} \\ &P_{in} - P_{load} = 6.79 \text{ mw (Experiment)} \end{aligned}$$

which agrees very closely.

It is concluded from this method that there is very little loss due to unwanted frequencies in this device and that the experimental device is functioning satisfactorily.

Simplified Circuit Loss Diagram

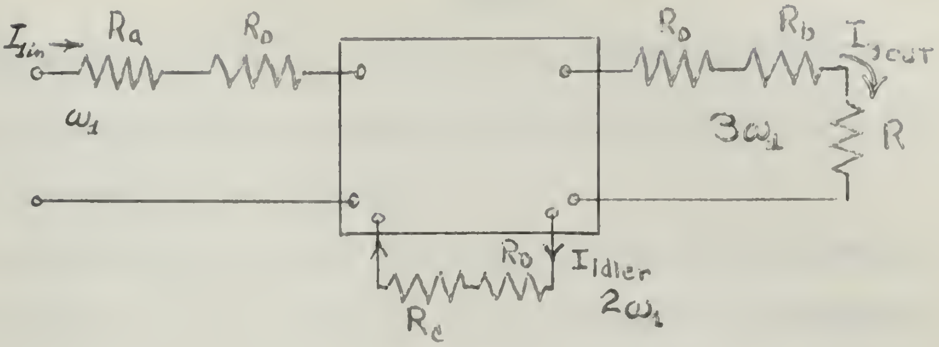

Figure 14

From figure 14 above it is noted that the input and output currents and the circuit loss can be measured, but the idling current cannot be measured. The perturbation method can be used, however, as long as the idling circuits losses are small. This is again an approximation method. First assume the idle current for the lossless case as determined from the Hamiltonian analysis, then apply this current to the losses in the idling circuit to determine the power lost.

This method will be used below to account for the power dissipated in the experimental multiple conversion circuit.

$$P_{1in} = \underset{\text{Fundamental}}{P_{loss}} + \underset{\text{idler}}{P_{loss}} + \underset{\text{output}}{P_{loss}} + P_{load}$$

For the optimum operating condition $P_{1in} = 13.5$ mw

$P_{3\ out} = 7.71$ mw

Circuit losses are as follows (figure 14)

$R_a + R_D = 24$

$R_b + R_D = 19$

$R_c + R_D = 19$

6

Summary

The multiple conversion process is an effective method of harmonic generation for the case where direct conversion is small due to the nonlinearity coefficients.

The experimental circuit developed for the problem operated satisfactorily and is a suitable circuit for the tests conducted. It is efficient as a direct conversion 2nd harmonic generator and as a multiple conversion 3rd harmonic generator.

The experimental circuit has shown potential as a two frequency output device and leads to possible practical application.

The theory as presented in section 3 gives greater insight into the energy characteristics and circuit relationships of nonlinear reactance harmonic generation. Further experimentation is needed to more thoroughly correlate with the theory.

7

Suggested Further Investigations

a) Obtain diodes with a larger 3rd order nonlinearity and conduct this same basic experiment to determine if multiple conversion is effective in this case. Particular attention should be given to the problem of phasing of the direct and multiple conversion energy.

b) Obtain more data on input impedance of this device to see if a more satisfactory correlation with theory can be obtained. The construction of a suitable fundamental matching circuit to be included in the work.

c) Use the same device and the same nonlinear elements and add a 4th and/or 5th harmonic circuit to determine conversion efficiency and further feasibility of the multiple frequency output device.

d) Design, build, and evaluate a microwave nonlinear reactance multiple conversion harmonic generator.

BIBLIOGRAPHY

(1) A. W. Swago, "Frequency Multiplier Circuits" Technical Report No 3 for U. S. Atomic Energy Commission, Contract No AT(11-1 - 392 Electrical Engineering Lab.; Engineering Experimental Station; University of Illinois, Urbana, Illinois.

(2) W. C. King, "Millimeter Wave Spectroscopic Components" Trans. of I.R.E., PGMTT, Vol MTT-2, No 3 p 13-16 Sept 1954.

(3) C. M. Johnson, "Superheterodyne Receiver for the 100 to 150 KMC Region" Trans. of IRE, PGMTT, Vol MTT-2, No. 3 P 27-32.

(4) S. E. Miller, "Waveguide as a Communications Medium", The Bell System Technical Journal, Vol. 33, No. 6, p 1209 - 1265.

(5) J. R. Fontana and H. J. Shaw, "Harmonic Generation at Microwave frequencies Using Field-Emission Cathodes", Proc. IRE, Vol 46, No. 6, p 1307, June 1958.

(6) H. C. Torrey and C. A. Whitmer, "Crystal Rectifiers", Radiation Laboratory Series, Vol. 15, McGraw Hill, New York, 1948.

(7) Shoichi Kita, "A Harmonic Generator by Use of the Nonlinear Capacitance of a Germanium Diode", Proc. of IRE, Vol. 46, No. 6, p 1307, June 1958.

(8) A. Uhlir, "The Potential of Semi-Conductor diodes in high frequency Communications" Proc. of IRE, Vol. 46, pp 1099-1115, June, 1958.

(9) M. M. Fortini and J. Vilms, "Solid State Microwave Power Source" Digest of Technical Papers, 1959 Solid State Circuits Conference, pp 82-85; February 12 and 13, 1959.

(10) C. H. Page, "Frequency Conversion with Ideal Rectifiers" Proc. IRE, Vol. 46, pp 1738-1740; October 1958.

(11) J. M. Manley and H. E. Rowe, "Some General Properties of Nonlinear Elements - pt I, General Energy Relations" Proc. IRE Vol. 44, pp 904-913; July 1956.

(12) K. K. N. Chang, "Harmonic Generation with Nonlinear Reactance", RCA Rev. Vol. 19, pp 455-464, Sept 1958.

(13) D. I. Breitzer, R. Gardner, J. C. Greene, P. P. Lombardo, R. Salzberg, K. Siegel., "Third Quarterly Progress Report Application of Semiconductor Diodes to Low Noise Amplifiers, Harmonic Generators, and Fast Acting TR Switches" Rept. No. 4589 - I-3; Contract: AF 30(602)-1854, Proj. No. 4589. Airborne Inst. Laboratory. pp 10-22, dtd March 1959.

(14) D. I. Breitzer, etc, "Fifth Quarterly Progress Report Application of Semiconductor Diodes to Low Noise Amplifiers, Harmonic Generators, and Fast Acting TR Switches", Rept. No. 4589 - I - 5; Contract: AF 30(602)-1854, Proj. No. 4589, Airborne Inst. Laboratory, pp C-1 to C-11, Sept. 1959.

(15) D. B. Leeson and S. Weinreb, "Frequency Multiplication with Nonlinear Capacitors -- A Circuit Analysis", Proc. IRE, Vol. 47, No. 12 pp 2076-2084, Dec. 1959.

(16) P. A. Sturrock, "Nonlinear Circuits Treated by Hamiltonian Methods" Unpublished technical paper prepared for Varian Associates dtd Dec. 1959 and addendum on same subject dtd March 1960.

(17) A. Uhlir, Jr. "Applications of New and Recently Developed Diodes", Technical Paper printed by Microwave Associates Inc., pp 9-13, 1959.

(18) H. Margenau and G. M. Murphy, "The Mathematics of Physics and Chemistry", pp 199-204, Van Nostrand, 1947.

(19) M. F. Gardner and J. L. Barnes, "Transients in Linear Systems", Vol. I, pp 60-85, Wiley 1947.

Appendix I

LARGE-SIGNAL ANALYSIS OF NONLINEAR REACTANCE HARMONIC GENERATOR (3RD HARMONIC) [13]

A large-signal analysis is being made of the operation of the abrupt-junction variable-capacitance diode as a harmonic generator. The specific problem considered is that of maximizing the power delivered by the diode at a particular harmonic frequency subject to the limitation that operation must be restricted to the region between reverse breakdown and forward conduction. Thus far, results have been obtained for the generation of third-harmonic power under the assumption that the diode is open-circuited at all harmonic frequencies higher than the third.

The abrupt-junction diode is chosen for investigation because of the mathematical simplicity of its voltage-charge characteristic--the instantaneous voltage v across the diode is a quadratic function of the instantaneous charge q stored in the diode. Because of this simple relation, it proves more convenient to discuss the operation of the abrupt-junction diode in terms of charge (or, alternatively, current) rather than voltage or impedance. Thus, the procedure followed is

1. To determine the current waveform for which the third-harmonic power output is a maximum.
2. To determine the voltages that must be impressed across the diode and the impedances that must be presented to the diode at the various harmonic frequencies in order that the current will have the desired optimum waveform.

The charge-voltage characteristic of the abrupt-junction diode is

described by the equation

$$q = -2A\sqrt{v_0 - v} \tag{1}$$

or inversely,

$$v = v_0 - \frac{q^2}{4A^2} \tag{2}$$

In equations 1 and 2, v_0, and A are constants whose values for any given diode can be determined experimentally by measuring the incremental capacitance C of the diode as a function of v. From equation 1

$$C = \frac{dq}{dv} = \frac{A}{\sqrt{v_0 - v}} \tag{3}$$

Let $-v_1$ denote the voltage at which the diode begins to conduct in the forward direction and $-v_2$ the voltage at which the diode breaks down in the reverse direction. Let $-q_1$ and $-q_2$ denote the corresponding values of q and C_1 and C_2 the corresponding values of C. Then, equations 1, 2, and 3 are valid only for

$$-v_2 < v < -v_1$$

$$-q_2 < q < -q_1$$

$$C_2 < C < C_1$$

If the diode is operated as a harmonic generator, q and v will be periodic functions of time and can be expanded into simple Fourier series. If, in particular, the diode is open-circuited at all harmonics higher than the third,

$$q = Q_0 + 2Q_1 \cos(\theta + \alpha_1) + 2Q_2 \cos(2\theta + \alpha_2) + 2Q_3 \cos(3\theta + \alpha_3) \tag{4}$$

In equation 4, $\theta = \omega_1 t$ where ω_1 is the fundamental radian frequency; Q_0, Q_1, Q_2, and Q_3 are the amplitudes of the d-c, fundamental,

second-harmonic, and third-harmonic components of charge; and α_1, α_2, and α_3 are phase constants.

The time derivative of equation 4 is the Fourier series representing the instantaneous current i flowing through the diode. By substituting equation 4 into equation 2 and using simple trigonometric transformations, we obtain the Fourier series representation of v. Finally, by, inspection of the series for i and v, we determine P_1, P_2, and P_3, the powers absorbed by the diode at fundamental, second-harmonic, and third-harmonic frequencies. The results obtained are

$$P_1 = \frac{\omega_1}{A^2}\left(p_{12} + p_{123}\right) \tag{5}$$

$$P_2 = \frac{\omega_1}{A^2}\left(-p_{12} + p_{123}\right) \tag{6}$$

$$P_3 = \frac{\omega_1}{A^2}\left(-3p_{123}\right) \tag{7}$$

where

$$p_{12} = Q_1^2 Q_2 \sin \phi \tag{8}$$

$$p_{123} = Q_1 Q_2 Q_3 \sin \psi \tag{9}$$

$$\phi = 2\alpha_1 - \alpha_2 \tag{10}$$

$$\psi = \alpha_1 + \alpha_2 - \alpha_3 \tag{11}$$

Two interesting observation can be made about the results expressed in equations 5 through 11. The first observation concerns the applicability of the Manley-Rowe relations to the harmonic generator. If the total power absorbed by a variable capacitance at each harmonic frequency is considered--that is P_1, P_2, and P_3 in the present case-- the Manley-Rowe relations reduce to an expression of the conservation of power-- that is, $P_1 + P_2 + P_3 = 0$ as can be seen by summing equations

5, 6, and 7. No information is furnished about the manner in which power is shared among the various harmonics. Equations 5, 6, and 7 shed some light on the reason for the lack of such information. These equations show that power conversion in a variable-capacitance harmonic generator can be considered as the result of several possible modes of power exchange. In each such mode, the division of power among the various harmonics involved is completely prescribed by the appropriate Manley-Rowe relation. However, the relative importance of the various modes depends on the external circuitry.

In the case of the abrupt-junction variable-capacitance harmonic generator, only two types of power-transfer modes are possible because of the simple quadratic voltage-charge characteristic of this type diode. The first type of mode can be called a "doubler" mode because it involves an exchange of power between two frequencies, one of which is twice the other. The second type of mode can be called a sum-frequency mode because it involves the exchange of power by three frequencies, one of which is equal to the sum of the other two. In the present case, where the diode current contains only fundamental, second and third-harmonic components, there is only one mode of each type present, namely the doubler mode p_{12} and the sum-frequency mode p_{123}. In the general case, where the diode current contains harmonics of all orders, there will be (1) a doubler mode p_{xy} for every pair of frequencies f_x and f_y, such that $f_y = 2f_x$, and (2) a sum-frequency mode for every combination of three frequencies f_x, f_y, and f_z, such that $f_z = f_x + f_y$.

The second observation about the results expressed in equations 5 through 11 concerns the existence of a scaling rule for the power converted in an abrupt-junction diode. For a given current waveform --

that is, for fixed values of the amplitude ratios, Q_2/Q_1 and Q_3/Q_1, and phase differences, ϕ and -- the power converted by the diode is proportional to the cube of the current amplitude and is independent of the bias. The word current is underlined to emphasize the point that scaling is applicable to the current through the diode and not the voltage across the diode. The scaling rule applies not only to the case under consideration but also to the more general case where higher-order harmonic components of current are allowed to flow through the diode. This rule has its origin in the quadratic voltage-charge characteristic of the abrupt-junction diode.

As a result of the scaling rule, maximizing P_3 subject to the restriction $-q_2 < q < -q_1$ is equivalent to maximizing the ratic $R = P_3/(\Delta q)^3$, where [1]

$$\begin{aligned}\Delta q &= q_2 - q_1 \\ &= 2C_2(v_0 + v_2)\left[1 - \sqrt{\frac{v_0 + v_1}{v_0 + v_2}}\right]\end{aligned} \qquad (12)$$

The mathematical details of the solution of this problem are presented in the Appendix. (13) The results obtained are as follows.

There are two "free"[2] stationary values of R. However, each of these two solutions requires that power be supplied to the diode not only at the fundamental but also at the second harmonic frequency. These solutions are not as interesting for practical reasons as solutions

---

[1] From Equations 1, 2, and 3.

[2] The designation "free" indicates that the values concerned are stationary for unconstrained variations of the independent variables.

that require a source of power only at fundamental frequency-- that is, solutions for which $P_2/P_3 \gtreqless 0$. Now the last inequality defines a region in the four-dimensional space of the variables Q_2/Q_1, Q_2/Q_1, ϕ, and ψ The only free stationary values of R lie outside this region. Consequently, the maximum value of R subject to $P_2/P_3 \gtreqless 0$ must lie on the boundary of this region. The problem therefore reduces to the determination of the stationary values of R subject to the constraint $P_2 = 0$. There are two solutions to the last problem and these yield apparently equal values of R.

The first solution is

$$q = Q_0' - \Delta q\left[0.310 \sin\theta + 0.168 \sin 2\theta + 0.155 \sin 3\theta\right] \tag{13}$$

$$i = -\omega_1(\Delta q)\left[0.310 \cos\theta + 0.355 \cos 2\theta + 0.466 \cos 3\theta\right] \tag{14}$$

$$Q_0' = -C_2(v_0 + v_2)\left[1 + \sqrt{\frac{v_0 + v_1}{v_0 + v_1}}\right] \tag{15}$$

Plots of q and i are given in Figure 12 and 13. The power converted by the diode from fundamental frequency to third-harmonic frequency is

$$P_3 = 0.0242\, \omega_1 C_2 (v_0 + v_2)^2 \left[1 - \sqrt{\frac{v_0 + v_1}{v_0 + v_2}}\right]^3 \tag{16}$$

It is interesting to note that this maximum rate of energy transfer is approximately equal to 0.04 W units of energy per fundamental period, where W denotes the energy required to charge the diode capacitance from an initial voltage $-v$, to a final voltage $-v_2$. The input impedance of the diode at fundamental frequency consists of a capacitive reactance, $1/\omega_1 C_{in}$, in series with a resistance, R_{1in}, where

$$\frac{1}{C_{1in}} = \frac{1}{2}\left(\frac{1}{C_2} + \frac{1}{C_1}\right)$$ (17)[1]

$$R_{1in} = 0.126\left[\frac{1}{\omega_1 C_2} - \frac{1}{\omega_1 C_1}\right]$$ (18)[2]

Thus, if $C_2 \ll C_1$, the loaded diode presents a Q of about 4 at a fundamental frequency. The second-harmonic termination is an inductive reactance $1/(2\omega_1 C_{in})$; and the third-harmonic termination is an inductive reactance, $1/(3\omega_1 C_{in})$, in series with a resistance

$$R_{3\ load} = \frac{4}{9} R_{1in}$$ (19)[3]

Note that the second-and third-harmonic terminations are in series resonance with the diode capacitance C_{in} at their respective frequencies.

[1] This is a linear approximation to the VvsC Characteristic curve

[2] R_{1in} is the real part of v/i using solution equations 13 and 14 at ω_1

[3] $R_{3\ load}$ is the real part of v/i from equation 13 and 14 at ω_3. Equation 19 is the resulting ratio of R_{1in} and R_{3load}.

Appendix II

Evaluation of Diode V vs C Characteristics

The voltage vs capacitance characteristics of the [8] V-33 and [2] V-20 Varicap Diodes* available for the experiment were measured on the Boonton R-X meter at a frequency of 1MC using the following circuit.

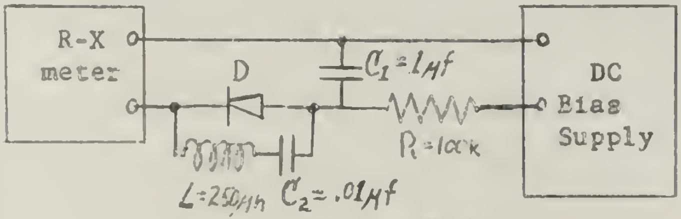

Figure II-A

The auxiliary coil, L, was necessary to bring the diode capacitance values within the range of measurement of the R-X meter. C_1 and C_2 are capacitors in the circuit to maintain the D. C. bias on the diode.

The bias voltage was varied from 0 to 20 and C was measured directly on the R-X meter. Table II-A is the tabulated data from these measurements.

Figure II-1 is this data averaged for the 8 V-33 and 2 V-20 Varicaps and plotted on a linear curve.

Figure II-2 is this data averaged for the 8 V-33 Varicaps and plotted as a log curve to show the coefficient of the V-C non-linearity.

---

*Manufactured by Pacific Semiconductor Co.

TABLE II-A

Voltage vs Capacitance for Varicap Diodes

Vbias	#1	#2	#3	#4	#5	#6	#7	#8	Avg 1to8	#9	#10
0	77.2	77	79	82	80	82.2	82.2	87	83		
0.5	56.0	53.5	55.5	58.7	54.7	57.0	56.5	61.2	55.8	44.2	42.2
1.0	46.5	45.5	46.2	48.9	46.5	48.3	47.5	52.2	47.7	37.2	35.2
1.5	40.5	40.2	40.9	43.6	40.7	42.6	41.7	44.9			
2.0	37.1	36.0	37.3	39.2	37.2	38.4	39.3	40.7	38.1	29.6	29.2
2.5	33.3	33.0	34.1	36.6	33.1	35.0	35.2	37.5			
3.	31.9	30.2	31.8	33.7	31.2	32.5	33.0	35.9	32.4	25.8	24.9
4	27.0	28.3	28.8	30.6	27.2	29.3	30.2	31.6		22.9	21.5
5	25.6	25.2	26.2	26.5	25.5	26.6	26.8	28.7	26.4	20.9	20.3
6	23.7	23.5	23.9	25.0	22.7	24.3	24.7	26.3		17.3	18.2
8	20.1	20.4	20.2	22.0	20.6	21.3	21.0	22.4	21.0	15.7	15.5
10	18.9	18.7	19.0	19.8	18.7	18.9	19.0	20.0	19.1	14.6	14.2
14	16.4	16.1	16.0	17.0	15.9	16.85	16.5	17.8	16.6		
18	14.1	14.1	14.4	14.4	13.9	14.4	14.4	16.1	14.4		
22					13.2	13.2		13.2			

ALL V-33 Varicaps

V-20 Varicaps

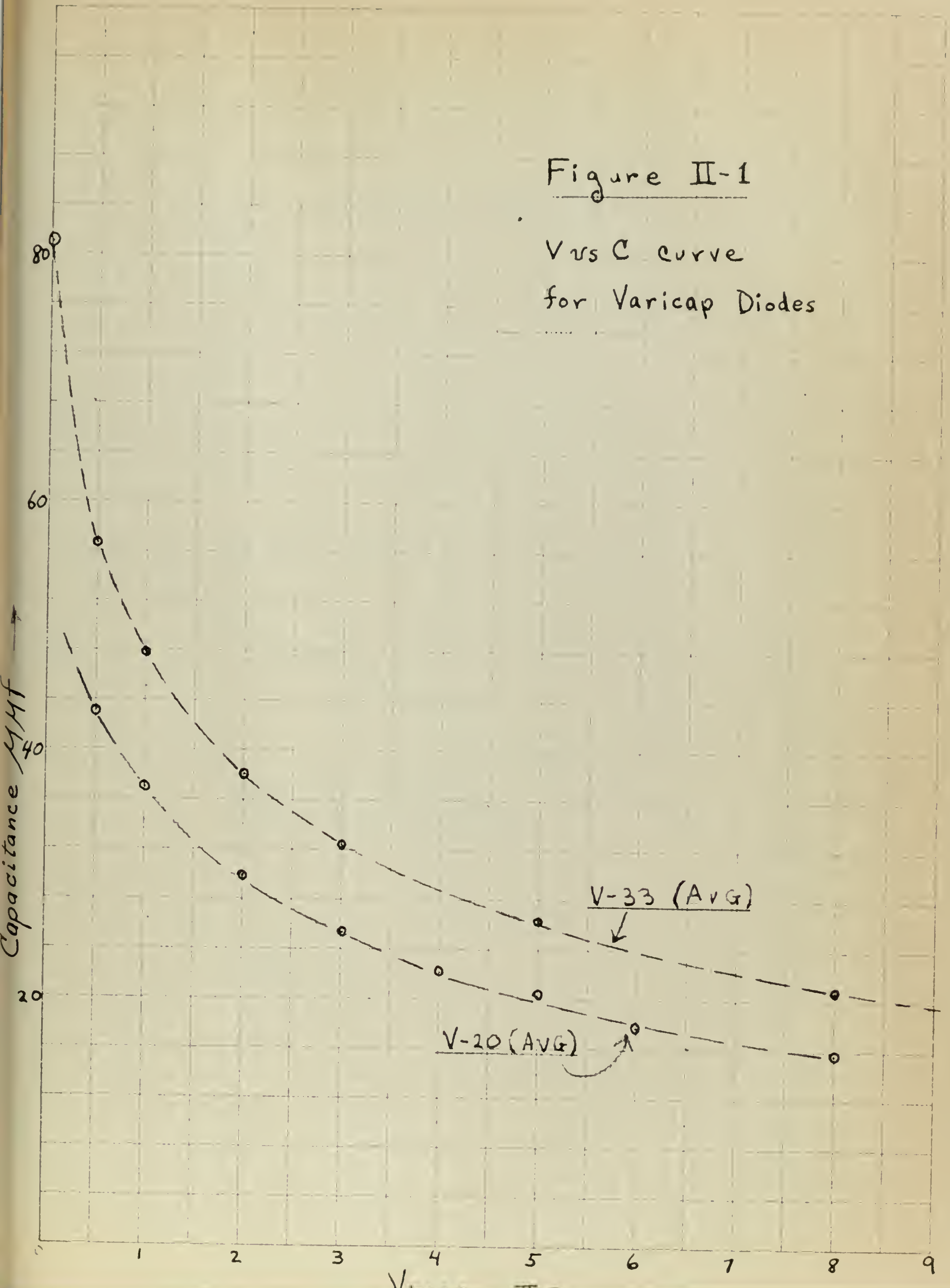

Figure II-1

V vs C curve for Varicap Diodes

Figure II-2

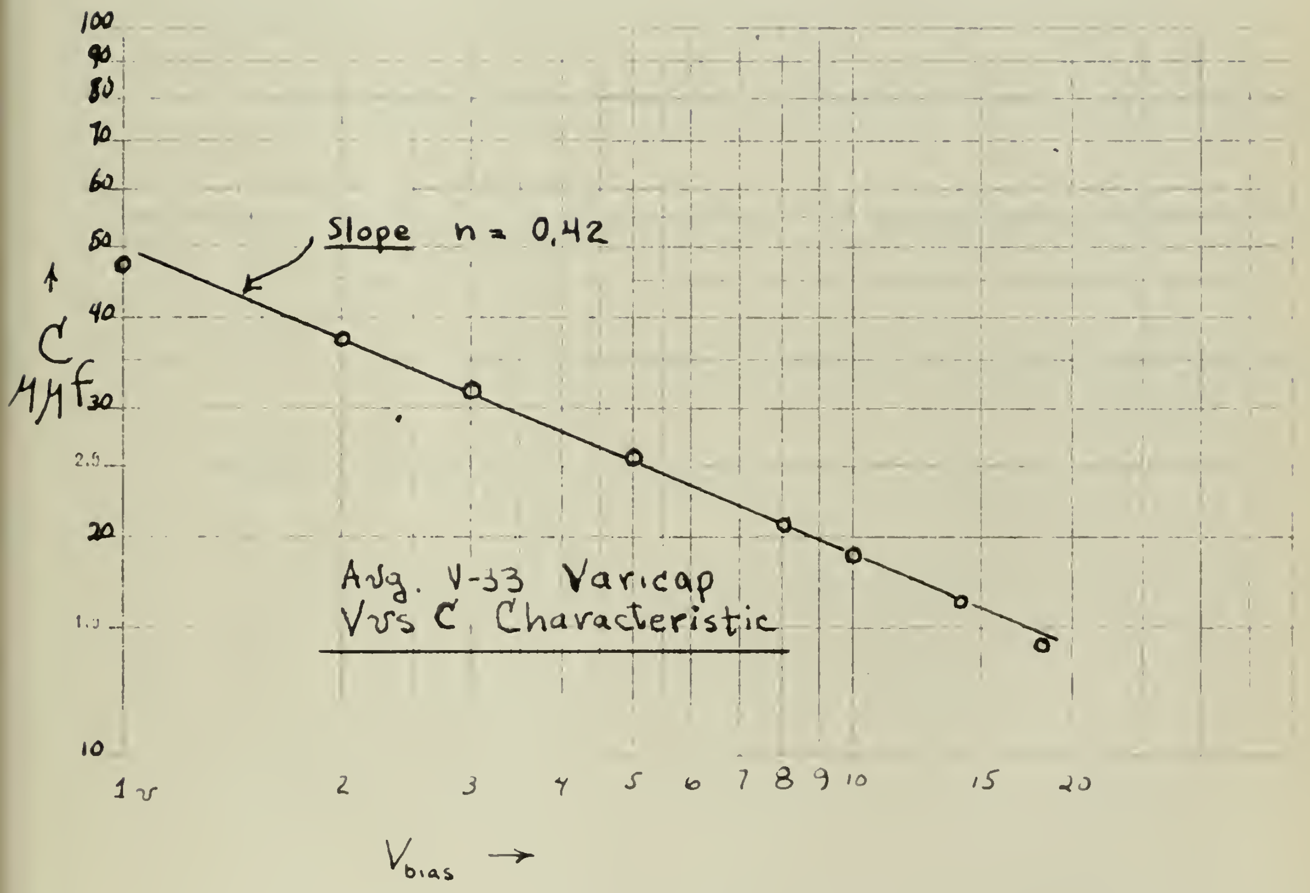

Slope n = 0.42

Avg. V-33 Varicap
V vs C Characteristic

Appendix III

Evaluation of Diode Energy vs Charge Characteristic

$$U = \frac{QV}{2}$$

$$Q = \frac{c_1}{1-n} V^{1-n} \qquad \therefore V = \left(\frac{1-n}{C_1}\right)^{\frac{1}{1-n}} Q^{\frac{1}{1-n}} \quad [15]$$

$$\therefore U = \frac{1}{2}\left(\frac{1-n}{C_1}\right)^{\frac{1}{1-n}} Q^{\frac{2-n}{1-n}}$$

Expressing U as a Taylor's Series expanded about Q_0 we get

$$U = f(Q) = f(Q_0) + (Q-Q_0) f'(Q_0) + \left(\frac{Q-Q_0}{2!}\right)^2 f''(Q_0) + \left(\frac{Q-Q_0}{3!}\right)^3 f'''(Q_0) + \dots$$

$$= \frac{1}{2}\left(\frac{1-n}{C_1}\right)^{\frac{1}{1-n}} Q_0^{\frac{2-n}{1-n}} + \frac{1}{2}\left(\frac{1-n}{C_1}\right)^{\frac{1}{1-n}}\left[\frac{2-n}{1-n}\right](Q-Q_0) Q_0^{\frac{1}{1-n}}$$

$$+ \frac{1}{2}\left(\frac{1-n}{C_1}\right)^{\frac{1}{1-n}}\left[\frac{2-n}{(1-n)^2}\right]\frac{(Q-Q_0)^2}{2!} Q_0^{\frac{n}{1-n}} + \frac{1}{2}\left(\frac{1-n}{C_1}\right)^{\frac{1}{1-n}}\left[\frac{n(2-n)}{(1-n)^3}\right]\frac{(Q-Q_0)^3}{3!} Q_0^{\frac{2n-1}{1-n}} + \dots$$

Setting n = .417 and $c_1 = 585.6 \times 10^{-12}$ this becomes

$$U \doteq 1.359 \times 10^{15} Q_0^{2.7153} + 3.690 \times 10^{15} (Q-Q_0) Q_0^{1.715} + 3.165 \times 10^{15} (Q-Q_0)^2 Q_0^{0.7153}$$

$$+ 0.7545 \times 10^{15} (Q-Q_0)^3 Q_0^{-0.2847} + \dots$$

Letting $Q_0 = 3.845 \times 10^{-9}$, the value of Q at V = 10, we get

$$U = 1.922 \times 10^{-8} + 13.645 (Q-Q_0) + 3.028 \times 10^{9} (Q-Q_0)^2 + 1.817 \times 10^{17} (Q-Q_0)^3 + \dots$$

$$U = \frac{1}{2}\left(\frac{1-n}{c_1}\right)^{\frac{1}{1-n}} Q^{\frac{2-n}{1-n}}$$

$$Q = \frac{c_1}{1-n} V^{1-n}$$

Figure III-1

Energy vs Charge Characteristi
of
Nonlinear Element used in
Harmonic Generator Circuit
(8 V-33 & 2 V-20 Varicap)

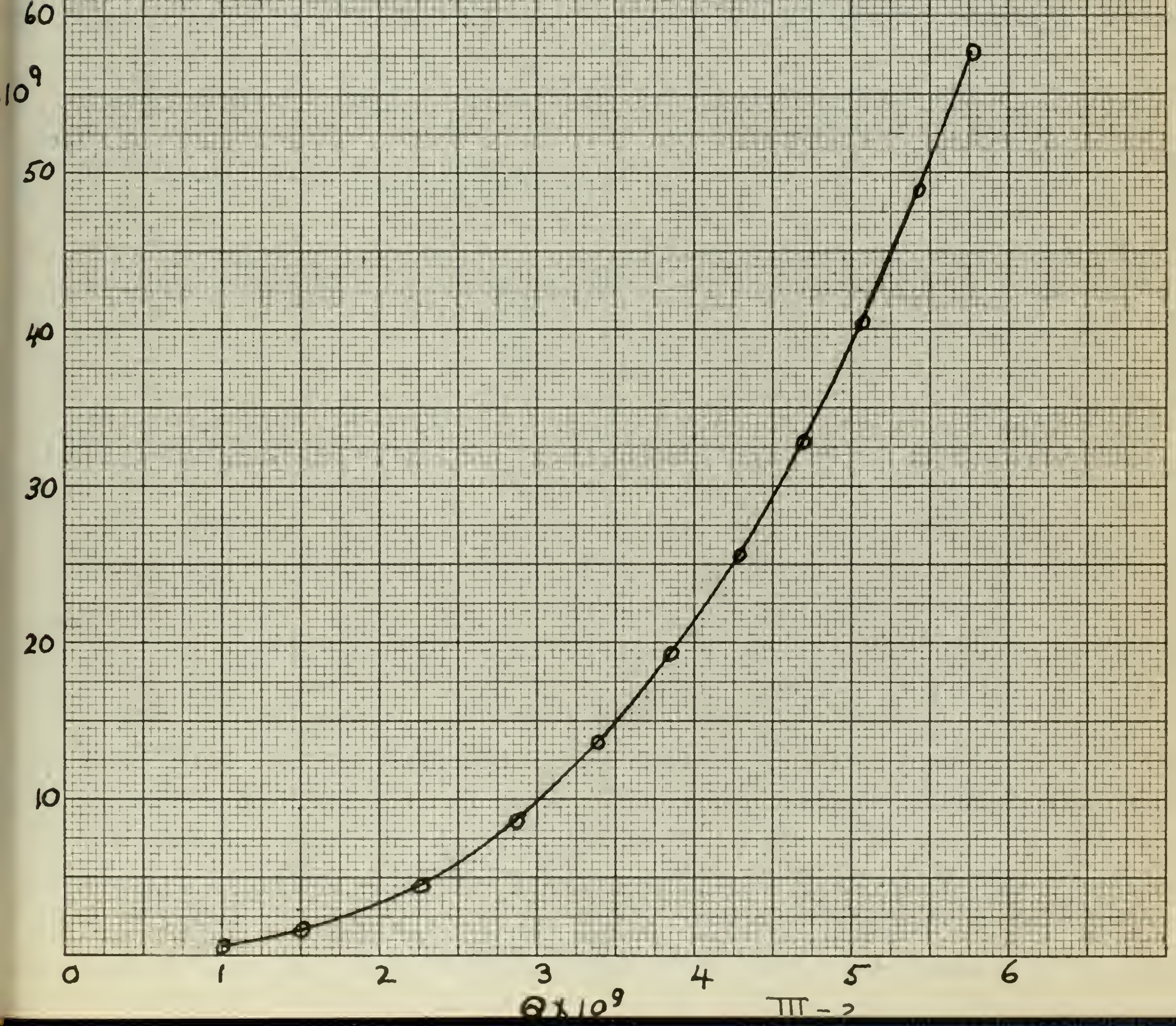

$$Q = \frac{c_1}{1-n} V^{1-n}$$

$$U = \frac{1}{2}\left(\frac{1-n}{c_1}\right)^{\frac{1}{1-n}} Q^{\frac{2-n}{1-n}}$$

Figure III-2

Energy and Charge
vs
Voltage Characteristic
of
Nonlinear Element used

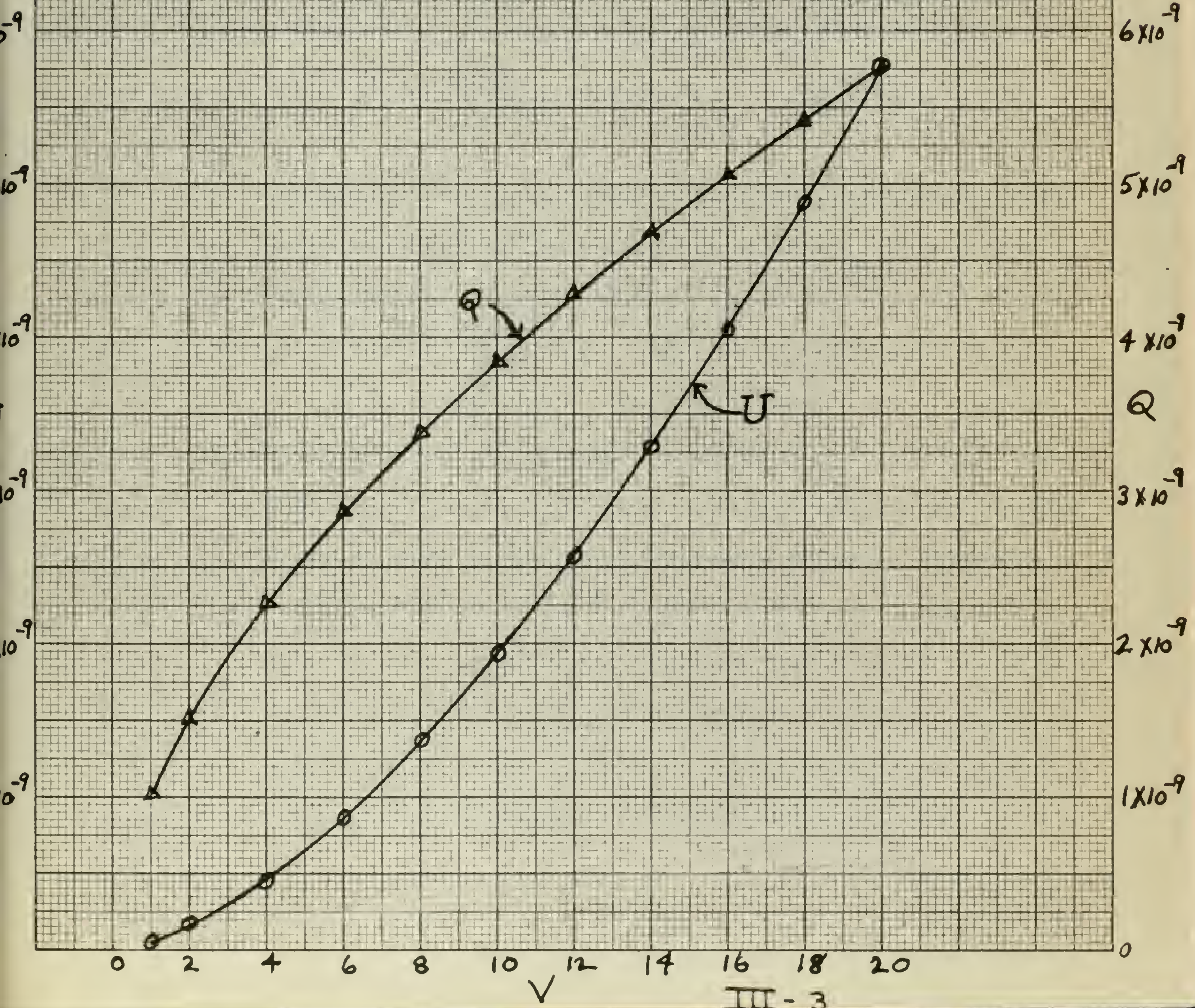

Appendix IV

A. Circuit Design Problems

1. Determination of C_{eff} using 8 V-33 and 1 V-20 Varicap.

   a) From equation 17 Appendix I

$$\frac{1}{C_{eff}} = \frac{1}{2}\left(\frac{1}{C_1} + \frac{1}{C_2}\right)$$

$$C_1 = 722\,pf \quad C_2 = 122\,pf \left\{ \begin{array}{l} \text{Calculated from data} \\ \text{Appendix II} \end{array} \right.$$

$$C_{eff} = 209\,pf$$

   b) From Reference 15

$$C_o = \frac{C_1}{V_o^{\gamma}} \qquad \left. \begin{array}{l} C_1 = 558\,pf \\ \gamma = 0.417 \end{array} \right\} \text{App. II}$$

$$C_o = \frac{558}{10^{(0.417)}} = 218\,pf \qquad V_o = 10\,v$$

2. Determination of R_{3L} (optimum) to be used in the bandpass filter calculations and for comparison with optimum R_{3L} from experiment (using equation 18 and 19 Appendix I.)

$$R_{1in} = \frac{0.126}{\omega_1}\left(\frac{1}{C_2} - \frac{1}{C_1}\right) = 136\ ohms$$

$$R_3 = \frac{4}{9} R_{1in} = 61\ ohms$$

3. Determination of the 3rd harmonic output filter. An image type band pass filter was used because of its simplicity and because it can be tuned if adjustable components are used. Therefore it was possible to change R_{3L} and to adjust the filter such that the input impedance was resistive and the filter pass band was still centered around the 3rd harmonic frequency. Standard handbook image BP filter equations were used with $R_o = R_{3L} = 61$ ohms and the 3db bandpass of ± 0.25 MC centered at 3MC.

4. Determination of series resonant trap components

L_A, C_A, and L_B, C_B

All components discussed refer to figure 5 section 4. The determination of L_A and L_B was a function of the impedances that these series trap circuits would present at the fundamental frequency at point A. Since both circuits are to be resonant at frequencies above the fundamental, they will be capacitive at the fundamental frequency. If this were a small capacitive reactance it would shunt the nonlinear element; therefore it was chosen to be very large. In this series type circuit to do this requires that C_A and C_B be small and L_A and L_B be as large as possible. This also means that we are adding losses to the circuit since the inductors are far from perfect though the Q's are fairly high.

The largest appropriate air core inductance available was the 260μh B.W. Miniductor with a Q at 1 MC of about 250.

5. Determination of L_1

Because of the series trap circuits as shown in Figure 5, L_1 was determined from a solution of the following circuit:

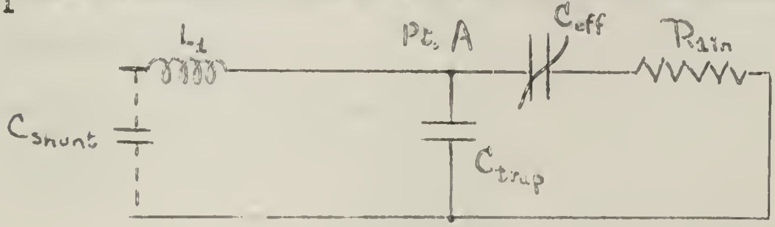

Figure IV-A

L_1 is the inductance necessary to resonate with C_{eff} and the shunting C_{trap} of the trap circuits at the fundamental frequency.

6. The input matching problem.

It was at this point in the design that a matching network was decided upon. The π network was to be used to match the 50 ohm output of the HP606A RF signal generator used in the experiment to the circuit.

This was done by solving for a mean resistance, R_m, at the input of L_1 such that

$$50 \text{ ohms} < R_m < R_{1\ in} \quad (136 \text{ ohms})$$

This comes from the quadratic solution for L_1 to resonate with the C_{eff}, $R_{1\ in}$, and C_{trap}.

With this input, $R_m + j0$, an L matching section was designed to match R_m to 50 ohms.

This completed the π matching network design, but due to lack of adequate equipment to measure for the matched condition it was discarded. It is suggested that in further work with this circuit, the matching network be rebuilt and an RF bridge oscillator with a sufficient driving voltage -- such as a GR 1330 -- be used with a compatible bridge circuit to insure a desireable impedance match.

7. Determination of L_2 and L_3

Basically $L_2 = \frac{1}{{}_2^{2}\, C_{eff}}$

and $L_3 = \frac{1}{{}_3^{2}\, C_{eff}}$

if the impedance levels of the two circuits are large at the other frequencies. That is, L_2 is not affected by L_3, etc

But it was found that this was not the case. Therefore, parallel tank circuits were added in the 2nd and 3rd harmonic output circuits and in the fundamental trap circuits to make the three frequency circuits independent. In all cases air core coils were used to keep losses low. It is suggested that the L's used in all cases be as small as possible to reduce losses.

3. Addition of 4th or 5th harmonic circuits to extend the multiple conversion process.

To convert this experimental device to a 4th or 5th harmonic generator is not difficult. Design of the additional circuit would be similar to that of the Multiple Conversion 3rd Harmonic Generator. It would require additional filters in all circuits to prevent undesirable frequency interaction due to low impedance levels. The 4th or 5th harmonic output circuits would be added at point B, and the additional series resonant trap circuits would be added at point A.

Appendix IV

B. Alignment Procedure for 2nd and 3rd Harmonic Generator Circuit.

1) Equipment required:

1 RF signal generator- frequency range 1 to 3 MC preferably with a crystal frequency calibrator such as HP606A.

1 VTVM with good frequency response in this range.

1 RF Bridge (for band-pass filter alignment).

Aligning procedure refers to circuit diagram Figure 5 page Frequency of signal generator and bridge signal was calibrated prior to using. Figure IV-1 is a photograph showing the circuit and the equipment used in the experiment.

2) Tuned series resonant circuits using the signal generator as a voltage source. Adjusted capacitor of L-C combination for a voltage maximum at the junction of the L and C at the specified frequency.

a. Aligned series resonant circuits as follows:

frequency	elements
1 MC	C_{C3}
2 MC	L_A C_A
3 MC	L_B, C_B

3) Tuned parallel resonant tank circuits using the signal generator as a current source by putting a large resistor in series. It may be necessary to disconnect each circuit and align it separately.

a. Aligned parallel resonant tank circuits as follows:

frequency	elements
2 MC	L_{3C}, C_{3C}
	L_{C1}, C_{C1}
3 MC	L_{C2}, C_{C2}
	L_{2A}, C_{2A}

4) Aligned 3MC band-pass filter at desired load R_{3L} using RF bridge such that filter input is $R_{3L} + j0$ by adjusting controls C_{3A} and C_{3B} on the filter section.

5) Alignment of 2MC output circuit.

Applied 10v back bias to the diode. Applied 2MC signal at point A. The 3MC output circuit should be disconnected at Point B. Adjusted C_2 for maximum signal at point B with $R_{2L} = 0$. Marked the setting of C_2. Thus this tuned the C_{eff} of the diode with L_2 for series resonance at 2 MC

6) Alignment of 3MC output circuit.

The idea here is basically the same as (5) above except that L_3 is the only tuning element available and therefore this was a "cut and try" procedure until alignment was attained.

This completes the circuit alignment.

7) Circuit operation

Bias 10

RF input adjusted until V_1 voltage across diode = 7.07v rms. measured at point A.

8) Power measurement method.

Placed small known resistor, r, in series with device; measured voltage point b to ground to obtain input power. Output power was measured across R_{3L} or R_{2L} to ground.

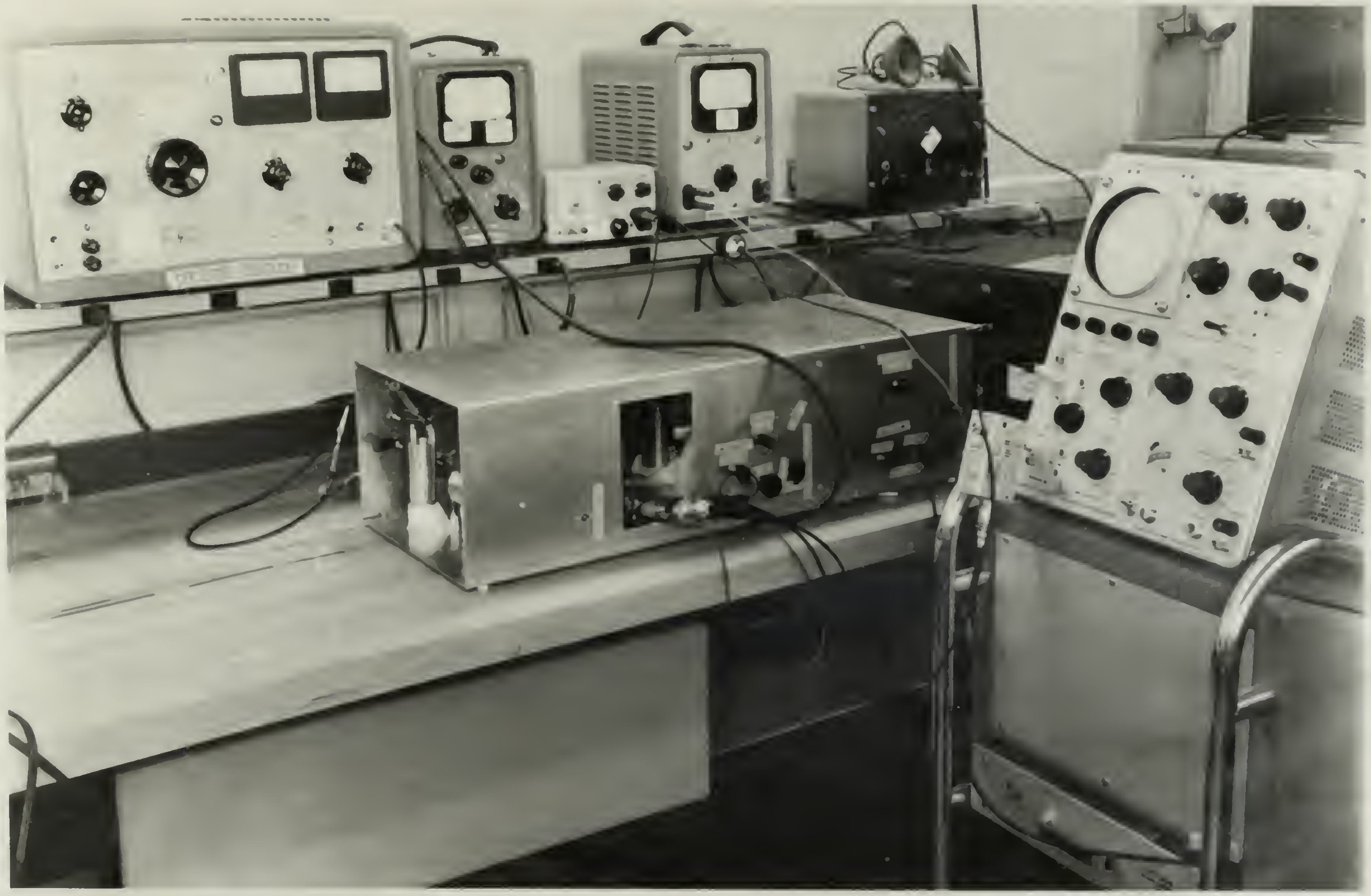

PHOTO COURTESY VARIAN ASSOC

HARMONIC GENERATOR AND TEST EQUIPMENT USED

FIGURE IV-I

APPENDIX V EXPERIMENTAL DATA

A. DIRECT CONVERSION DATA

R_{2L} ohms	V_1 volt(rms)	$P_{1(in)}$ mw	$P_{2(out)}$ mw	P_1/P_2 db	Vbias Volts-dc
50	7.07	8.15	4.04	3.04	10
100	7.07	7.78	4.58	2.3	10
100	6.60	6.67	3.74	2.52	10
125	7.07	6.30	3.95	2.02	10
130	7.07	7.07	4.84	1.65	10
150	7.07	7.02	5.28	1.24	10
150	6.0	4.34	2.99	1.62	10
150	5.0	2.48	1.5	2.18	10
200	7.07	6.32	4.57	1.41	10
300	7.07	5.9	3.96	1.81	10
300	6.0	3.24	2.11	1.86	10
300	5.0	1.52	0.99	1.8	10
300	4.0	0.9	0.48	2.7	10
300	3.0	0.38	0.14	4.3	10

R_{3L} ohms	V_1 Volts(rms)	$P_{1(in)}$ mw	$P_{3(out)}$ mw	P_1/P_3 db	Vbias Volts-dc
50	7.07	1.68	2.3	28.5	10
60	7.07	1.53	6.5	23.0	10
80	7.07	1.7	2.5	28.0	10

B. Multiple Conversion Data

R_{3L} ohms	V_1 volts, rms	P_1 mw	P_3 mw	P_1/P_3 db	Vbias volts-dc	R_{2L} ohms	P_2 mw	R_{1in} (Calc)
45	7.07	13.1	6.92	2.76	10	0		
45	6.00	9.22	4.6	3.00	10	0		
45	5.25	6.55	2.95	3.45	10	0		
45	4.5	4.5	1.68	4.28	10	0		
45	3.5	2.23	0.59	5.76	10	0		
50	7.07	12.6	6.85	2.64	10	0		98
50	7.07	12.6	5.3	3.8	10	50		
50	7.07	1.52	14μw	20.4	10	10K		
50	7.07	1.46	5.7μw	24.1	10	Large Reactance		
60	7.07	14.4	7.93	2.58	10	0		111
60	7.07	12.9	5.95	3.4	10	50	2.31	
60	5.25	7.4	3.16	3.68	10	0		
60	4.5	4.57	1.86	3.88	10	0		
60	3.5	2.16	0.6	5.56	10	0		
70	7.07	13.5	7.71	2.42	10	0		124
70	7.07	15.1	6.23	3.87	10	50	2.45	
70	7.07	1.45	4.87μw	24.7	10	10K		
70	7.07	(Effect same as 50)			10	Large Reactance		
80	7.07	14.6	8.15	2.54	10	0		112
80	6	11.3	5.46	3.1	10	0		
80	5.25	7.87	3.79	3.18	10	0		
80	5.0	6.8	3.24	3.22	10	0		
80	4.5	4.95	2.18	3.54	10	0		
90	7.07	12.25	5.65	3.36	10	0		112
90	7.07	14.8	5.9	4.00	10	50	2.74	
90	7.07	1.73	26μw	18.2	10	10K		
100	7.07	16.6	7.7	3.34	10	0		110
100	7.07	13.5	5.7	3.74	10	50		
100	7.07	1.45	9.4μw	21.9	10	10K		
100	6.0	12.35	5.81	3.28	10	0		
100	5.25	8.85	3.9	3.4	10	0		
100	5.0	6.93	3.1	3.5	10	0		
100	4.5	5.59	2.11	4.2	10	0		
100	3.5	2.47	0.738	5.28	10	0		